EVALUATION OF PERVIOUS CONCRETE MIXES IN AREAS SUBJECT TO SNOW PLOW OPERATIONS AND ABRASIVE AND SALT APPLICATION

Draft Final Report

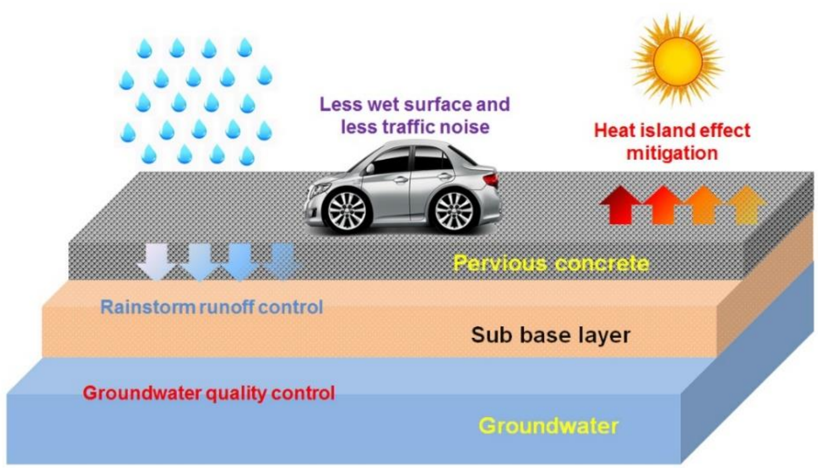

July 2014

EVALUATION OF PERVIOUS CONCRETE MIXES IN AREAS SUBJECT TO SNOW PLOW OPERATIONS AND ABRASIVE AND SALT APPLICATION

Draft Final Report

by

Ning Xie, Ph.D.
Stephen Mery
Yudong Dang, Ph.D.
Michelle Akin, P.E.
Xianming Shi, Ph.D., P.E.

Western Transportation Institute
College of Engineering
Montana State University
PO Box 174250
Bozeman, MT 59717

for

Nevada Department of Transportation
Research Section
Attn: Manju Kumar
1263 S. Stewart Street
Carson City, NV 89712

and

Federal Highway Administration
400 Seventh Street, SW
Washington, DC 20590-0003

July 2014

Technical Report Documentation Page

1. Report No.	2. Government Accession No.	3. Recipient's Catalog No.

4. Title and Subtitle	5. Report Date
EVALUATION OF PERVIOUS CONCRETE MIXES IN AREAS SUBJECT TO SNOW PLOW OPERATIONS AND ABRASIVE AND SALT APPLICATION	July 2014
	6. Performing Organization Code
7. Author(s) Ning Xie, Stephen Mery, Yudong Dang, Michelle Akin, Xianming Shi	8. Performing Organization Report No.
9. Performing Organization Name and Address Corrosion and Sustainable Infrastructure Lab Western Transportation Institute P. O. Box 174250, Montana State University Bozeman, MT 59717-4250	10. Work Unit No. (TRAIS) 11. Contract or Grant No.
12. Sponsoring Agency Name and Address Nevada Department of Transportation Research Section 1263 S. Stewart Street Carson City, NV 89712 and Federal Highway Administration 400 Seventh Street, SW Washington, DC 20590-0003	13. Type of Report and Period Covered 14. Sponsoring Agency Code

15. Supplementary Notes

16. Abstract

This research serves to evaluate an important stormwater management tool that would help the Nevada Department of Transportation (NDOT) comply with state and federal regulations in reducing the fine sediment load from State roadways. NDOT needs effective tools to meet recently enacted federal (EPA) regulations for reducing the amount of fine sediment generated from NDOT right-of-way within the Lake Tahoe basin. In the summer of 2012, NDOT began constructing a pervious concrete pavement near Lake Tahoe. Specifications for this installation included a 7″ thick pervious concrete pavement surface over an 8″ thick aggregate drainage layer and 6″ thick geotextile-encapsulated sand bed. This project provided an opportunity to conduct laboratory tests and monitor field sites, so that NDOT could learn from these applications and implement pervious concrete effectively in other areas. This work encompassed a case study of two pervious concrete installations at SR 431 and SR 28, with both pre- and post-construction QA testing. In addition to a comprehensive literature review, field investigation was supplemented by laboratory investigation to assess whether the pervious concrete sections installed by NDOT would be durable and effective under normal winter maintenance operations.

The mechanical properties (compressive strength, splitting tensile strength, and abrasion resistance) of the pervious concrete samples cored from SR28 were better than those from SR431. The samples cored from SR28 exhibit slightly higher density and lower air void content than those from SR431, and they also feature lower hydraulic conductivity and water absorption and better resistance to salt scaling than those from SR431. The micro X-Ray Computed Tomography (μCT) analysis illustrates that the micrometer-scale porosity of the samples cored from SR28 was much lower than those from SR431.

A forensic investigation was conducted to shed light on the premature raveling of some pervious concrete segments. For cores from both pervious concrete sections, the scanning electron microscope (SEM) observations reveal that the samples with limited distress feature a well-maintained cement binder phase, whereas those with moderate distress feature some needle-shape precipitates embedded in the cement binder phase and those with severe distress feature a large amount of micro-sized crystalline precipitates instead of cement binder phase. The specific mechanism responsible for the premature failure of pervious concrete remains unclear and merits further investigation. One hypothesis to test is that the distresses observed in pervious concrete originated from the construction practice, e.g., insufficient compaction at some locations, and later aggravated by the exposure to freeze/thaw cycles, deicers, and mechanical loading in the service environment.

17. Key Words	18. Distribution Statement
Pervious concrete; filed investigation; infiltration rate; SEM; properties; microstructure analysis;	

19. Security Classification (of this report)	20. Security Classification (of this page)	21. No. of Pages	22. Price
Unclassified	Unclassified		N/A

Technical Report Form DOT F 1700.7 (8-72) Reproduction of completed page authorized Printed on recycled paper

SI* (MODERN METRIC) CONVERSION FACTORS

APPROXIMATE CONVERSIONS TO SI UNITS

Symbol	When You Know	Multiply By	To Find	Symbol
		LENGTH		
in	inches	25.4	millimeters	mm
ft	feet	0.305	meters	m
yd	yards	0.914	meters	m
mi	miles	1.61	kilometers	km
		AREA		
in^2	square inches	645.2	millimeters squared	mm^2
ft^2	square feet	0.093	meters squared	m^2
yd^2	square yards	0.836	meters squared	m^2
ac	acres	0.405	hectares	ha
mi^2	square miles	2.59	kilometers squared	km^2
		VOLUME		
fl oz	fluid ounces	29.57	milliliters	ml
gal	gallons	3.785	liters	L
ft^3	cubic feet	0.028	meters cubed	m^3
yd^3	cubic yards	0.765	meters cubed	m^3
		MASS		
oz	ounces	28.35	grams	g
lb	pounds	0.454	kilograms	kg
T	short tons (2000 lb)	0.907	megagrams	Mg
		TEMPERATURE (exact)		
°F	Fahrenheit	(F-32)/1.8	Celsius	°C

NOTE: Volumes greater than 1000 L shall be shown in m^3.

APPROXIMATE CONVERSIONS FROM SI UNITS

Symbol	When You Know	Multiply By	To Find	Symbol
		LENGTH		
mm	millimeters	0.039	inches	in
m	meters	3.28	feet	ft
m	meters	1.09	yards	yd
km	kilometers	0.621	miles	mi
		AREA		
mm^2	millimeters squared	0.0016	square inches	in^2
m^2	meters squared	10.764	square feet	ft^2
m^2	meters squared	1.196	square yards	yd^2
ha	hectares	2.47	acres	ac
km^2	kilometers squared	0.386	square miles	mi^2
		VOLUME		
ml	milliliters	0.034	fluid ounces	fl oz
L	liters	0.264	gallons	gal
m^3	meters cubed	35.315	cubic feet	ft^3
m^3	meters cubed	1.308	cubic yards	yd^3
		MASS		
g	grams	0.035	ounces	oz
kg	kilograms	2.205	pounds	lb
Mg	megagrams	1.102	short tons (2000 lb)	T
		TEMPERATURE (exact)		
°C	Celsius	1.8C+32	Fahrenheit	°F

*SI is the symbol for the International System of Measurement

ACKNOWLEDGMENTS

The authors acknowledge the financial support for this project provided by the Nevada Department of Transportation (NDOT). They appreciate the guidance provided to this project by the NDOT project manager Manjunathan Kumar and panel members Tyler J. Thew, Matthew L. Nussbaumer, Darin P. Tedford, Kelly H. Yokotake, and Andrew E. Knust. They also acknowledge Kevin Senn and Dick Minto of Nichols Consulting Engineers (NCE) for providing the infiltration rates and pavement distresses data mentioned in Chapter 4 and Marie Venner of Venner Consulting and Carla Little of Western Transportation Institute for editorial review.

DISCLAIMER

Table of Contents

List of Figures

List of Tables

Chapter 1 Introduction

1.1 Problem Statement

Pervious concrete has been increasingly used as a powerful tool to mitigate watershed impacts due to stormwater runoff. It also has positive effects on urban heat island mitigation and ground water purification. Pervious concrete pavements have an open network of pores to allow infiltration through the pavement with a subsequent reduction in the quantity of stormwater runoff and an improvement in water quality (total suspended solids, total phosphorous, total nitrogen, and metals (McCain, 2010)). This is achieved via mechanical and biological mechanisms. A typical pervious concrete mix design used in the U.S. consists of cement, single-sized coarse aggregate (between 1″ and the No. 4 sieve), and a water/cement ratio between 0.27 and 0.43. The various mixes can feature a wide range of properties, e.g., effective air voids of 14 to 31%, permeability of 35–800 in/hr, and compressive strength of 800-3,000 psi (Schaefer, 2006).

However, there are some issues of concern which must be addressed when using pervious concrete. Proper mixing and installation is necessary to ensure appropriate in-place material characteristics. Large void spaces in pervious concrete significantly affect the mechanical properties of the material; as a result, it is important to maintain a proper balance between infiltration capacity and the mechanical properties of the materials. Furthermore, winter road maintenance can have a large influence on the longevity and effectiveness of a pervious concrete installation. Heavy metal mobilization by deicers and sedimentation of abrasives can lead to expensive maintenance or stormwater management issues. Seasonal freeze-thaw cycling due to deicer use can also pose a significant risk to pervious concrete durability. In addition, clogging can reduce the effectiveness of pervious concrete and special maintenance techniques are generally needed to restore performance, such as sweeping and/or vacuuming. Clogging can occur due to a variety of actions, including traction sand applied during winter storms, sediments in stormwater from adjacent land that intersects the roadway configuration, and collapsed pores from vehicle traffic (McCain, 2010).

The Nevada Department of Transportation (NDOT) needs effective tools to meet recently enacted federal (EPA) regulations for reducing the amount of fine sediment generated from NDOT right-of-way within the Lake Tahoe basin. Infiltration is the most effective method of reducing fine sediment. In place of impervious surfaces, pervious concrete pavement reduces runoff and distributes infiltration. In the summer of 2012, NDOT began constructing a pervious concrete pavement near Lake Tahoe. Specifications for this installation included a 7″ thick pervious concrete pavement surface over an 8″ thick aggregate drainage layer and 6″ thick geotextile-encapsulated sand bed. This project provided an opportunity to conduct laboratory tests and monitor field sites, so that NDOT could learn from these applications and implement pervious concrete effectively in other areas. This project encompassed a case study of two pervious concrete installations at SR 431 and SR 28. The studies included pre- and post-construction QA testing.

The research was part of an effort to identify tools that would help NDOT comply with state and federal regulations to reduce the fine sediment load from State roadways. In addition, research was needed to ensure pervious concrete installed by NDOT will be durable and effective under their normal winter maintenance operations.

1.2 Research objectives

The research objectives of this study were to assess the efficacy of pervious concrete in areas subject to snow plow operations and abrasive and salt application, in terms of managing quantity and quality of stormwater runoff. It investigated the durability and performance of pervious concrete (e.g., in void content, strength and hydraulic conductivity). To this end, the research team documented the laboratory and field performance of two pervious concrete pavement sections near Lake Tahoe in an effort to better understand the functionality and durability of such assets.

Performance and durability aspects of pervious concrete pavement are unique for different mixes. This project provided an opportunity to analyze NDOT installations of pervious concrete pavement to ensure acceptable performance. The laboratory testing simulated many years of field service and provided indications of performance and durability without waiting for the results from the field installations. It leveraged existing research to address a key knowledge gap for deploying pervious concrete pavements in cold regions where unique challenges exist.

1.3 Anticipated Benefits

This work is expected to produce substantial benefits for NDOT, county and city stakeholders, as well as agencies with similar climate, by understanding the efficacy and appropriateness of pervious concrete pavement, a Low Impact Development (LID) technology. Upon successful achievement of the project objective, a number of benefits can be expected:

1) Pervious concrete enables the use of space that is already part of the highway system for stormwater runoff control, thus reducing the need for additional land. Reducing the amount of impervious surfaces may reduce or prevent the need for other stormwater management infrastructure (e.g., ponds, wetlands, and vegetated swales and filter strips), by decreasing the volume, flow rate and contaminant loading in stormwater runoff. Other potential benefits include: reducing heat-island effect and pavement noise; reducing road salt application; reducing hydroplaning, glaring or other safety hazards due to water on pavements; and minimizing impact to the local ecosystem.

2) This research will likely facilitate the shift from impermeable pavement surfaces to permeable surfaces and promote the integration of eco-friendly pervious concrete design and construction into highways, parking lots, sidewalks, local roads, etc.

3) At this stage, the cost of implementation and ongoing operations and maintenance of pervious concrete pavement in Nevada is yet to be determined. However, relative to impervious concrete, pervious concrete pavement is anticipated to have similar cost, but larger savings in terms of increased pavement safety and mobility, improved level of service, and improved environmental stewardship. These benefits will be realized once pervious concrete pavement makes the transition from the *First Application (Contract) Field Pilot* Stage to the *Specification & Standards with Full Corporate Deployment* Stage and becomes widely adapted by NDOT for highway areas where stormwater runoff is a significant concern.

1.4 Scope of Work and Report Organization

To accomplish the proposed objectives, this work was designed to include multiple tasks as follows: (1) a comprehensive literature review to summarize the research of the current pervious concrete constructions, including the construction and maintenance methods, property testing and evaluation approaches, and unsolved problems; (2) a systematic laboratory investigation of the performance, including the compressive and splitting tensile strengths, abrasion resistance, air voids and water permeability, and freeze/thaw resistance in sodium chloride solution of the field pervious concrete samples; (3) microstructure analysis of these cored samples to elucidate the potential deterioration mechanisms. The following chapters present the NDOT case study on the pervious concrete pavement.

Chapter 2 will outline the methodology of the research conducted, specific to both laboratory testing and field investigations. It will describe the mechanic and forensic testing procedures and the standard methods by which they were conducted. It will also describe the in-situ evaluation performed on site. Chapter 3 will consist of a comprehensive assessment of the available literature pertaining to pervious concrete construction and its implementation, as well as an assessment of what research remains to be conducted in order to make accurate and informed decisions when choosing whether and how to integrate pervious concrete into a construction project. In chapter 4, a summary of the field investigations conducted by the Nevada Department of Transportation and Nichols Consulting Engineers will be presented. This will include a location report detailing the characteristics of the site and the results from the onsite performance evaluation. Chapter 5 will present the results of the laboratory investigation with respect to the mechanical properties and forensic assessment of pervious concrete samples from the two sites. An interpretation of those results will also be provided in order to create a more comprehensive view of what is happening in the field. Finally, a concluding summary will highlight the research findings in Chapter 6. Recommendations for the future implementation of pervious concrete under these conditions will be provided based on a comprehensive assessment of all the preceding information.

1.5 References

McCain, G.N., M.J. Suozzo, M.M. Dewoolkar. 2010. A Laboratory Study on the Effects of Winter Surface Applications on the Hydraulic Conductivity of Porous Concrete Pavements. Transportation Research Board 2010 Annual Meeting CD-ROM.

Schaefer, V.R., K. Wang, M.T. Suleiman, and J.T. Kavern. 2006. Mix Design Development for Pervious Concrete in Cold Weather Climates. Iowa DOT Final Report No. 2006–01.

Chapter 2 Methodology

2.1 Review of Previous Research

Prior to conducting testing, the research team reviewed and summarized existing knowledge related to laboratory testing of pervious concrete.

Permeability tests are frequently conducted in the laboratory on pervious concrete samples. While not yet standardized by ASTM or AASHTO, the most common type of laboratory test is a falling head permeability test (McCain, 2010; Huang, 2010; Rizvi, 2010; Schaefer, 2006). In this type of test, a sample is sealed on the sides; the researcher then records the amount of time for water applied to the surface of the sample to drop in height. The time and beginning and ending pressure head are used to compute hydraulic conductivity. Two options for testing the infiltration rate in the field include ASTM C1701, or a method developed and refined over several years by Minnesota DOT personnel (personal communication with Bernard Izevbekhai, MnDOT).

A demonstration project in Yakima, WA (Yakima County website) compared water samples collected from sample vaults in pervious concrete pavement and impervious (traditional) asphalt pavement. The pervious concrete water samples had significantly lower biochemical oxygen demand (2.5 vs. 11 mg/l), total suspended solids (25 vs. 320 mg/l), copper (8 vs. 20 μg/l), lead (0 vs. 20 μg/l), zinc (0 vs. 160 μg/l), #2 Diesel (0.4 vs. 1.4 mg/l), and motor oil (0.5 vs. 2.3 mg/l). Other examples of improvements to water quality are documented (McCain, 2010; and Brown-*presentation online*).

Pervious concrete pavements are reported to have improved skid resistance (McCain, 2010; and Izevbekhei, 2008), although little supporting data was found in a cursory search of literature. Tests in a Pennsylvania parking lot with pervious concrete using a British pendulum tester (ASTM E303) showed pervious concrete had similar skid resistance to traditional asphalt and porous asphalt (Houle, 2008).

The abrasion resistance of pervious concrete can be easily measured following ASTM C1747 using a Los Angeles abrasion machine with parameters specifically developed for pervious concrete. Wu et al. found adding styrene butadiene rubber (SBR) latex polymer to pervious concrete mixes significantly improved abrasion resistance, and although it decreased, had adequate permeability (Wu, 2010).

Schaefer et al. (Schaefer, 2006) found saturated freeze-thaw performance (using ASTM C666) could be improved by several different changes to the mix design: using a small amount of fine aggregate (sand), adding polypropylene fibers, using a slightly higher water/cement ratio, increasing compaction (lower porosity), including entrained air and increasing paste volume, replacing some Portland cement with fly ash or silica fume, or using a latex admixture (Kevern, 2008). Yang (2011) also found silica fume, polypropylene fibers, and/or increased cement content improved saturated freeze–thaw durability, particularly for water-cured specimens. Unclogged, unsaturated pervious concrete specimens tested for freeze–thaw resistance with ASTM C666 had significantly greater durability than either clogged and/or saturated specimens, with no significant differences in structural properties (Guthrie, 2010).

McCain et al. in Vermont found during a laboratory study that a large application of a sand-salt 2:1 (by weight) mixture at 0.24 lb/ft^2 (equivalent to 15,200 lb/lane-mile) reduced the hydraulic conductivity of laboratory-mixed pervious concrete specimens by about 15 percent. Adding sand to the surface and shaking the samples simulated maximum clogging and reduced the hydraulic conductivity by about 35 percent. Vacuuming the samples restored the hydraulic conductivity to about 90 percent of their initial values (McCain, 2010).

2.2 Methodologies

The samples for testing were cored from the sites SR431 and SR28. Table 2.1 gives the mixture proportions of the pervious concrete studied in this work. The designed void content is 25%, and the water-to-cement ratio is 0.29. The cement was Nevada type II, the aggregate specific gravity is 2.64, and the testing results and the NDOT specifications on the aggregates are shown in Table 2.2.

Table 2. 1 Mixture proportions of the pervious concrete in this work

Mixture Proportions - for 1 cubic yard			
Mixture Component	**Weight, lb**	**Volume (ft^3)**	**Volume (%)**
Cement	463	2.36	8.7%
SCM	82	0.55	2.0%
Coarse Aggregate, SSD	2441	14.82	54.9%
Sand, SSD	0		
Water	158	2.53	9.4%
Eucon DS, fl.oz.	54.5		
Eucon X15, fl.oz.	27.2		
Design Void Content, %		6.75	25.0%
Total weight, lbs	3144		
Total volume, ft^3		27.00	
Design Density, lb/ft^3		116.4	
Theoretical density (void free), lb/ft^3		155.2	

Table 2. 2 The testing results and the NDOT specifications of the aggregates

Sieve Size Analysis (ASTM C136/C117)		
	Percent By Weight Passing	
U.S. Standard Sieve Size	Paiute Pit	ASTM C33/NDOT Specification
½ Inch	100	100
⅜ Inch	100	85 - 100
No. 4	25	10 - 30
No. 8	2	0 - 10
No. 16	2	0 - 5
No. 200	0.9	0 - 1.0

2.2.1 Compressive Strength

Compressive strength performance was assessed based on the testing standard ASTM C39, adapted as follows given that an official standard has not been established for pervious concrete. Cores were cut to a height of eight inches for a diameter to height ratio of 0.5 and left to dry for 24 hours.

In order to ensure flat, parallel surfaces on the top and bottom of the sample, the cores were capped with cement in accordance with the recommended standard ASTM C617. The water to cement ratio of the neat cement paste was 0.3. A small quantity of water reducer was added such that the mixture was 1% reducer by mass. Using this cement mixture, a flat end of the core sample was pushed into the cement such that the full sample surface was covered by approximately 4 mm of cement. Excess cement paste was removed to avoid the cement capping extending beyond the circumference of the core. A set of levels was used to ensure that the cap surface was perpendicular to the axis of the cylindrical sample. The cement was left to harden for 6 hours before repeating the process for the opposite end of the sample.

Once the cement caps had dried completely, six measurements were recorded for the height of each sample. The cores were then compressed vertically at a rate of 440 lbs/s until failure. The maximum force applied to reach failure was recorded for each sample. Fig. 2.1 shows the images of the samples for compressive strength testing.

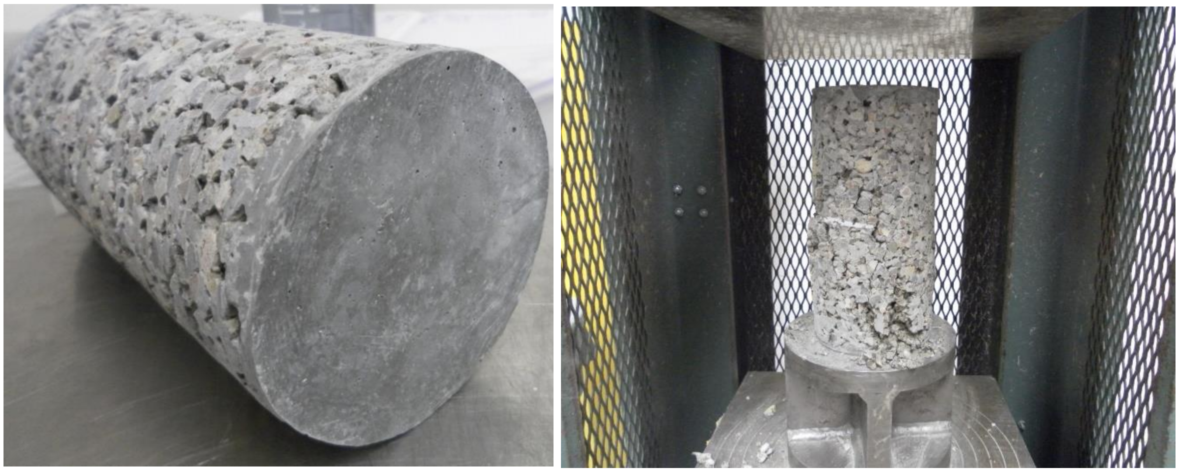

Fig. 2. 1 Samples for compressive strength test

2.2.2 Tensile Strength

Tensile strength performance was assessed based on the testing standard ASTM C496. The cores were cut to a height of eight inches for a diameter to height ratio of 0.5 and left to dry for 24 hours.

In order to ensure flat, parallel and stable surfaces for tensile strength testing, a cement strip was applied to opposite edges along the full length of each sample. This was done following the standard ASTM 617 for capping cylinders for compression testing, but with the application of the neat cement paste along the length of the samples in two diametrically opposite strips. The water to cement ratio of the paste was 0.3. A small quantity of water reducer was added such that the mixture was 1% reducer by mass. Using this cement mixture, one edge of the core sample was pushed into the cement such that the full sample length was covered by a strip of cement that was approximately 4 mm deep. The cement was left to harden for 6 hours before repeating the process for the opposite side of the sample. During the process, a set of levels was used to ensure that the cement surfaces were parallel to each other and perpendicular to the same diameter of the cylindrical core.

Once the cement strips had dried completely, six measurements were recorded for the height of each sample. The cores were then compressed along their diameter at a rate of 132 lbs/s until failure. The maximum force applied to reach failure was recorded for each sample. Fig. 2.2 shows the images of the samples for the splitting tensile strength test.

Fig. 2. 2 Samples for splitting tensile strength test

2.2.3 Density, Voids and Absorption

Density and void percentage were measured based on the testing standard ASTM C1754. The cores were prepared so that rough edges were shaved off with a saw to establish a more uniform height among a given set of samples.

Multiple diameter and length measurements were taken for each sample using calipers for the purpose of determining the density of the samples. The dry mass of each sample was determined using the drying method as follows. The mass of the sample was recorded before the sample was placed in an oven to dry for 24 hours at a constant temperature of 100 ^{0}C. After drying for 24 hours, the mass of the sample was again measured until the change in recorded mass for each sample was below 0.5% of the mass before that drying period. This condition was met after two drying periods.

The resulting mass for each sample was used with average length and diameter measurements to determine the sample density using the following equation

$$\text{Density} = \frac{K \times A}{D^2 \times L}$$

where:

A = the dry mass of the sample in grams
D = the average diameter of the sample in mm
L = the average length of the sample in mm
K = 1,273,240 is a correction factor with unit conversions to kg/m^3

The submerged mass of each sample was then determined by placing a water bath on a scale with a sample suspended in the bath. The sample was suspended by resting a wooden dowel across the rim of the bath and tying a string from the dowel to the center of the core. After leaving each sample in the water bath for 30 minutes, the sample was struck with a rubber mallet to dislodge any air bubbles remaining within the sample. Then the submerged mass and temperature of the water bath were recorded. The void content, as a percentage, was calculated using the following equation

$$\text{Void Content} = \left[1 - \left(\frac{K \times (A - B)}{\rho_w \times D^2 \times L}\right)\right] \times 100$$

where:

B = the submerged mass of the sample in grams
ρ_w = the density of water at the measured temperature of the water bath.

Water absorption was measured based on the testing standard ASTM C642. The dry mass of each sample was recorded and the sample was submerged in water for 24 hours. The sample was then removed from the water, allowed to drain, and patted dry on the exposed surfaces. The mass of the sample was measured again before it was placed in the water for another 24 hour period. This was repeated until the change in mass of the sample was less than 0.5% of the previous period. The water absorption was then calculated using the following formula

$$\text{Absorption (\%)} = \frac{(B - A)}{A} \times 100\%$$

where:

A = the initial, dry mass of the sample
B = the final mass of the sample after immersion.

2.2.4 Abrasion Resistance

Resistance to abrasion was evaluated based on the testing standard ASTM C1747. Each sample was cut to 4 inches in height and air dried for 36 hours. After drying, the sample masses were each measured and recorded.

Three samples corresponding to the same location group SR28 were placed in a Los Angeles Abrasion Testing Machine set to 500 revolutions at 30 revolutions per minute. All the resulting material was sifted through a 1 inch sieve and the material retained was recorded. The same process was then repeated for three samples from location SR431.

2.2.5 Water Permeability

An established standard does not currently exist in order to best determine the permeability of water in pervious concrete. However, previous research has had success adapting a falling head permeameter to measure the infiltration rate of water through pervious concrete samples. The testing method used here follows that used during previous research (McCain, 2010; Rizvi, 2010; and Schaefer, 2006).

A falling head test was performed on each of three samples from each sample location. Test samples were cut to 4 inches in height. The samples were sealed with silicone along the full height of the cylinder so that only the top and bottom faces of the sample were free to pass water though them.

A standpipe apparatus was fashioned from 4 inch nominal diameter PVC pipe. The standpipe design was modeled after that used by Schaefer (2006). Three pieces of pipe were cut for each standpipe: one piece 20 inches in length as the top standpipe tube and two pieces 4 inches in length. One of the 4 inch pieces was used as the bottom drainage reservoir. The other 4 inch piece housed the sample.

A 1.25 inch diameter hole was drilled in the bottom PVC piece as an outlet for the water. A thin plastic plate was attached to the bottom of the pipe with watertight silicone sealer. A second square plastic plate was fashioned with a 4 inch diameter hole in the center. Four holes were also drilled in the second plate, one in each of the outer quadrants of the plate. The second plate was then attached to the top of the bottom PVC piece so that the 4 inch hole matched that of the pipe.

The top PVC piece had a small hole drilled in it near the bottom. A small, clear plastic tube used to measure the water level inside the standpipe was inserted into this hole and attached, straight and vertical, to the outside of the standpipe. Intervals of one inch were then marked along the clear tube by measuring upwards from the bottom of the PVC piece to a height of 15 inches. A plastic plate identical to the plate fashioned for the top of the first 4 inch pipe was crafted and attached to the bottom of the top PVC piece.

The second 4 inch pipe was cut from top to bottom along a single length of the pipe to allow enough flexibility to insert the pervious concrete sample. After inserting the sample, the vertical opening of the pipe and the pipe-sample boundaries at the top and bottom were sealed with silicone. Fig. 2.3 shows the images of the water permeability testing preparation before testing.

The sample was then placed between the top and bottom portions of the standpipe apparatus with circular rubber spacers between. A nut and bolt was used for each of the four holes in the plastic plates. The boundaries between the top and bottom of the sample and its respective portion of the apparatus were sealed with silicone. Fig. 2.4 shows the water permeability testing apparatus.

A rubber stopper was placed in the outlet at the bottom of the apparatus and the standpipe filled with water to above the 15 inch mark. Using a stopwatch with repeatable lap capabilities, the rubber stopper was removed and a lap time recorded as the water level dropped to each inch interval. This process was performed three times for every sample.

Fig. 2. 3 Water permeability testing preparation

Fig. 2. 4 Water permeability testing apparatus

2.2.6 Salt Scaling

A drained test method was used to test for salt scaling resistance. A solution of 3% sodium chloride by mass was used for the experiment. The samples were slabs cut to 8.5 X 8.5 X 4 inches with two slabs from each location.

Clear plastic containers of an appropriate size were selected to hold the samples during the experiment. During the experiment, the container rested on top of another plastic container, which served as a reservoir into which the salt solution drained. Spacers were placed in the container between the sample and the container bottom to prevent the sample from lying in the pool of solution which remained after draining. Two small holes were drilled in the bottom of the container to allow the salt solution to drain out. These holes were sized so that the time it took for the sample to go from completely submerged to not at all submerged in the solution was approximately 20 minutes. Fig. 2.5 shows the images of the salt scaling testing process.

Each cycle of freezing and thawing began by placing the sample in the container on top of the spacers, filling the container with sodium chloride solution so that the sample was completely submerged, and placing the setup in the freezer. The drainage progress had to be checked every few minutes to make sure that the drainage holes were not clogged or frozen over.

Fig. 2. 5 Images of the salt scaling testing process

Samples remained in the freezer for 24 hours, at which time they were removed to thaw for another 24 hours. After thawing, the slabs were gently rubbed to remove any loose material and the mass of the slabs was measured. All material that scaled during the cycle was collected, oven-dried for 24 hours and measured for mass. The process was repeated for seven cycles, at which time severe scaling dictated the originally planned length of ten cycles be cut short.

2.2.7 Microstructure analysis

The low and high magnification fracture surfaces of the samples cored from sites SR431 and SR28, which were both divided as *limited*, *moderate*, and *severe*, respectively, were observed by scanning electron microscope (SEM) and X-ray tomography (μCT). SEM was conducted under an accelerating voltage of typically 20 kV. The resolution of the μCT analysis is 10 μm.

2.3 References

ASTM. 2012. Standard Test Method for Compressive Strength of Cylindrical Concrete Specimens. ASTM standard C39/C39M. American Society for Testing Materials, West Conshohocken, PA.

ASTM. 2011. Standard Test Method for Splitting Tensile Strength of Cylindrical Concrete Specimens. ASTM standard C496/C496M. American Society for Testing Materials, West Conshohocken, PA.

ASTM. 2012. Standard Practice for Capping Cylindrical Concrete Specimens. ASTM standard C617/C617M. American Society for Testing Materials, West Conshohocken, PA.

ASTM. 2006. Standard Test Method for Density, Absorption and Voids in Hardened Concrete. ASTM standard C642. American Society for Testing Materials, West Conshohocken, PA.

ASTM. 2012. Standard Test Method for Scaling Resistance of Concrete Surfaces Exposed to Deicing Chemicals. ASTM standard C672/C672M. American Society for Testing Materials, West Conshohocken, PA.

ASTM. 2011. Standard Test Method for Determining Potential Resistance to Degradation of Pervious Concrete by Impact and Abrasion. ASTM standard C1747/C1747M. American Society for Testing Materials, West Conshohocken, PA.

ASTM. 2012. Standard Test Method for Density and Void Content of Hardened Pervious Concrete. ASTM standard C1754/C1754M. American Society for Testing Materials, West Conshohocken, PA.

Brown, H.J. "Monitoring Pervious Concrete for Water Quality in a Laboratory and Field Environment" Presentation, online, http://www.rmc-foundation.org/images/PCRC%20Files/Hydrological%20&%20Environmental%20Design/Monitoring%20Pervious%20Concrete%20for%20Water%20Quality%20in%20a%20Laboratory%20and%20Field%20Environment.pdf

Guthrie, W.S., C.B. DeMille, D.L. Eggett. 2010. "Effects of Soil Clogging and Water Saturation on Freeze–Thaw Durability of Pervious Concrete" Transportation Research Board 2010 Annual Meeting CD-ROM.

Houle, K.M. 2008. Winter Performance Assessment of Permeable Pavements: A comparative study of porous asphalt, pervious concrete, and conventional asphalt in a northern climate. M.S. Thesis, University of New Hampshire.

Huang, B., H. Wu, X. Shu, and E.G. Burdette. 2010. "Laboratory Evaluation of Permeability and Strength of Polymer-Modified Pervious Concrete" *Constr. and Build. Mat.*, 24(5), 818–823.

Izevbekhei, B. 2008. "Pervious Concrete" TERRA Fact Sheet, November 2008.

Kevern J.T., Wang K., and Schaefer V.R. 2008. "Pervious Concrete in Severe Exposures" *Concrete International*, 30(7), July, 43–49.

McCain, G.N., M.J. Suozzo, M.M. Dewoolkar. 2010. "A Laboratory Study on the Effects of Winter Surface Applications on the Hydraulic Conductivity of Porous Concrete Pavements" Transportation Research Board 2010 Annual Meeting CD-ROM.

Rizvi, R., S. Tighe, V. Henderson, J. Norris. 2010 "Evaluating the Use of Recycled Concrete Aggregate in Pervious Concrete Pavement" *Transportation Research Record No. 2164*, 132-140.

Schaefer, V.R., K. Wang, M.T. Suleiman, and J.T. Kavern. 2006. Mix Design Development for Pervious Concrete in Cold Weather Climates. Iowa DOT Final Report No. 2006–01.

Wu, H., B. Huang, X. Shu, Q. Dong, E. Shrum, D. Jared, and P. Wu. 2010. "Laboratory Evaluation of Latex-Modified Pervious Concrete" Transportation Research Board 2010 Annual Meeting CD-ROM.

Yakima County website, Regional Stormwater Management Program, Project: Low Impact Development Demonstration Project, http://www.yakimacounty.us/stormwater/LID/project.htm.

Yang, Z. 2011. "Freezing-and-Thawing Durability of Pervious Concrete under Simulated Field Conditions" *ACI Materials Journal*, 108(2), March-April, 187–195.

Chapter 3 Pervious Concrete: State of the Knowledge

Pervious concrete has been increasingly used as a powerful tool to mitigate negative impact on the environment (Tennis, 2004; Offenberg 2005; Scholz, 2007; Joung 2008; Volder, 2009; Schaefer, 2011). It has many advantages to urban cities, including stormwater runoff management, traffic noise control, groundwater recharge, and mitigation of the urban heat island (Cackler, 2006; Wanielista, 2007; Lee, 2009; Schwartz, 2010; Garber, 2011; Haselbach, 2011; Ullate, 2011, Li, 2014). Figure 3.1 illustrates some of the main advantages of a pervious concrete pavement.

Pervious concrete pavements have an open network of pores to allow infiltration through the pavement with a subsequent reduction in the quantity of stormwater runoff and an improvement in water quality with respect to total suspended solids, phosphorous, nitrogen, and metals (McCain, 2010). This is achieved via mechanical and biological mechanisms. Specifications for a pervious concrete pavement constructed near Lake Tahoe in the summer of 2012 included a 7″ thick pervious concrete pavement surface over an 8″ thick aggregate drainage layer and 6″ thick geotextile-encapsulated sand bed. A typical pervious concrete mix design used in the U.S. consists of cement, single-sized coarse aggregate (between 1″ and the No. 4 sieve), and a water to cement ratio (W/C) between 0.27 and 0.43. The various mixes can feature a wide range of properties, e.g., effective air voids of 14 to 31%, permeability of 35-800 in/hr, and compressive strength of 800-3,000 psi (Schaefer, 2006). Clogging can reduce the effectiveness of pervious concrete, and special maintenance techniques are generally needed to restore performance, such as sweeping and/or vacuuming. Clogging can occur due to a variety of actions, including traction sand applied during winter storms, sediments in stormwater from adjacent land that intersects the roadway configuration, and collapsed pores from vehicle traffic (McCain, 2010).

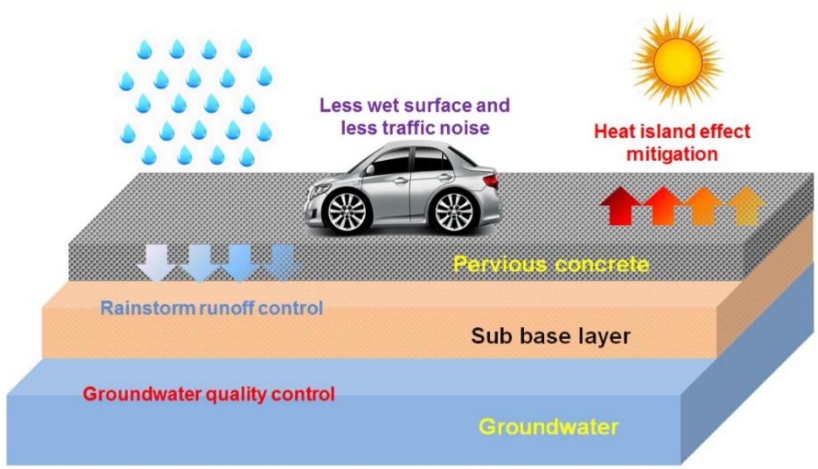

Fig. 3. 1 Schematic demonstration of the main advantages of pervious concrete pavements

In this chapter, recent studies on pervious concrete pavements are extensively summarized. First, the advantages of pervious concrete pavements are discussed from an environmental perspective, such as water quality control, recycling waste materials applications, heat island effect mitigation, and driving noise reduction; second, the design policies and implementation of the pervious concrete pavements are briefly discussed; third, the overall properties of the pervious concrete pavements, including the hydraulic and infiltration properties, mechanical properties, and abrasion resistance properties, are systematically reviewed; after that, the durability problems of the pervious concrete pavements, i.e. the freeze/thaw damages and clogging phenomenon are discussed, and in addition, the most widely applied maintenance methods are introduced as well; finally, the microstructure characterization of the pervious concrete through various advanced characterization approaches are reviewed. This information will help to optimize the design policies and performance of the implemented pervious concrete pavements. Figure 3.2 shows a flow diagram to illustrate the structure of this chapter.

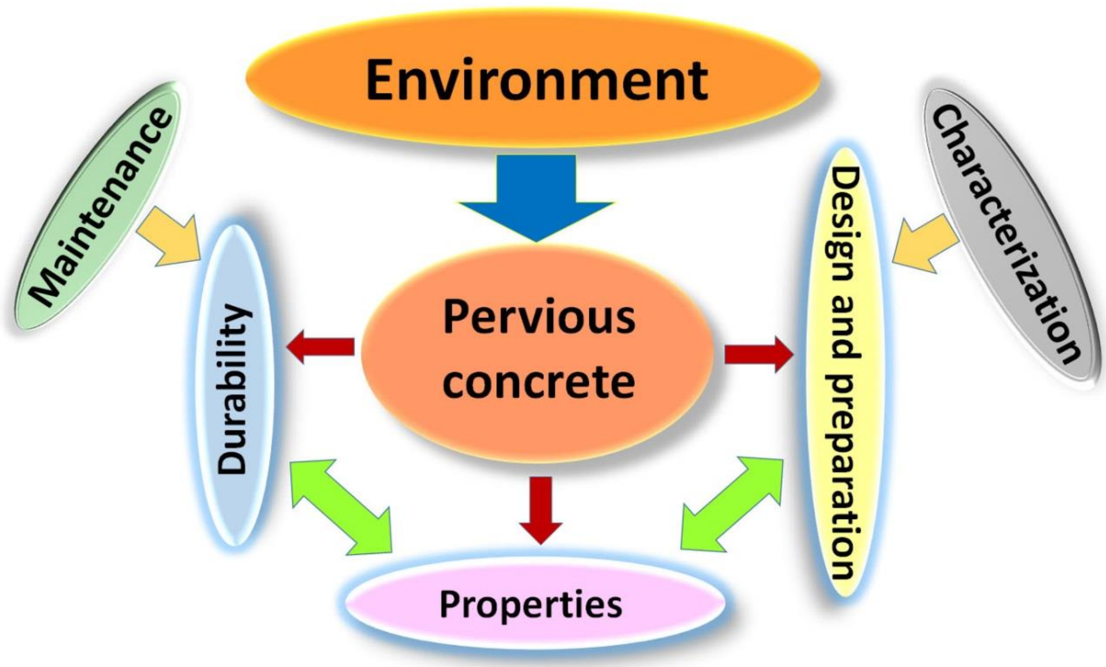

Fig. 3. 2 Pervious concrete considerations

3.1 Environmental Perspective

3.1.1 Stormwater runoff and water quality control

Two infiltrating low-impact development (LID) practices configured in-series, pervious concrete and bioretention (PC-B), were monitored for 17 months to examine the hydrologic and water quality response of this LID treatment train design (Brown RA, 2012). When compared with a single treatment practice (bioretention) that was monitored at the same site, the two LID practices in-series treated an additional 10% of annual runoff volume, discharged approximately one-half as much outflow volume, and discharged significantly lower peak outflow rates. However, the water quality results were not as promising because of the influx of groundwater in the bioretention cell and the lack of denitrifying conditions in either the bioretention cell or pervious concrete system.

A demonstration project in Yakima, WA (Yakima County website) compared water samples collected from sample vaults in pervious concrete pavement and impervious (traditional) asphalt pavement. The pervious concrete water samples had significantly lower biochemical oxygen demand (2.5 vs. 11 mg/l), total suspended solids (25 vs. 320 mg/l), copper (8 vs. 20 μg/l), lead (0 vs. 20 μg/l), zinc (0 vs. 160 μg/l), #2 Diesel (0.4 vs. 1.4 mg/l), and motor oil (0.5 vs. 2.3 mg/l). Other examples of improvements to water quality are documented (McCain, 2010 and Brown HJ).

The quality and quantity of residential stormwater runoff from a control, traditional and low impact development (LID) watershed were compared in a paired watershed study (Bedan ES, 2009). During the study, nitrate and nitrite-nitrogen (NO3 + NO2-N), ammonia-nitrogen (NH3-N), total Kjeldahl nitrogen (TKN), total phosphorus (TP), and total suspended solids (TSS) were analyzed weekly using flow-weighted and composites of stormwater. Total copper, lead, and zinc were analyzed monthly. Mean weekly storm flow increased 600 times from the traditional watershed in the post-construction period. Increased exports of TKN, NO3 + NO2-N, NH3-N, TP, Cu, Zn, and TSS in runoff were associated with the increased storm flow. Post-construction storm flow in the LID watershed was reduced by 42%, while peak discharge did not change from preconstruction conditions. Exports were reduced from the LID watershed for NH3-N, TKN, Pb, and Zn, while TSS and TP exports increased. Similar results indicated that the typical stormwater concentration of dissolved Cu and Zn can be removed effectively through a pervious concrete layer (Haselbach, 2014).

Best management practices (BMP) were studied on the campus of Villanova University (Kwiatkowski, 2007). It was found that copper and chloride were the two constituents of concern at this site. Copper was introduced to the system from a roof, while chloride was introduced from deicing practices. Copper was not found in pore water beneath 0.3 m and the chloride was not significant enough to impact the ground water. This research indicates that with proper sitting, an infiltration BMP will not adversely impact the ground water.

A similar project monitored infiltration-based stormwater best management practices (BMP) for a commercial development site in Aurora, Colorado (Earles TA, 2008). Total precipitation for the year of 2007 was relatively close to historical averages; however, during certain months the totals were much greater than historical average conditions. Water quality inflow into BS-IN appears to have higher concentrations of most analyzed pollutants than BS-IS. There was little surface runoff that left the monitored portion of the site, indicating that most runoff was infiltrated onsite by the “experimental”

BMPs monitored. Concentrations from the one sample event where all of the samplers triggered indicate a large percent removal of pollutants from the influent verses the effluent for all the parameters monitored.

The impact of glyphosate-containing herbicide (GCH) on pollution attenuation and biodegradation in pervious paving systems was studied most recently (Mbanaso 2013). It was concluded that the GCH stimulated high numbers of oil degrading bacteria and fungi. The protists could be immediately killed by GCH but recovered within a week. The taxonomic richness could be reduced and the responses of the protists may allow the development of a bio-indicator system for GCH. The GCH negated the trapping and retention of hydrocarbons by the geotextile, and the herbicide reduced the capacity of the geotextile to trap metals in the pervious pavement system.

The soil moisture and chemical properties of pavements were analyzed by Morgenroth (2007, 2013). It was demonstrated that the soil moisture and aeration dynamics differ greatly beneath paved and unpaved surfaces; differences are usually insignificant between pervious and impervious paving. If urban trees do benefit from overlying pervious paving relative to impervious paving it is probably not a consequence of soil moisture or aeration. The pavement style changed the pH value of the soil from 5.75 to 6.3. The effect on pH was higher beneath porous pavements when a gravel base was included. Concentrations of Al, Fe, and Mg decreased, while Na increased beneath pavements. Soil moisture was consistently higher beneath pavements than control plots, except following periods of heavy rainfall where high soil moisture muted all treatment effects.

Some studies of pervious concrete pavement working as a photocatalyst by mixing TiO_2 with the cementitious material have been performed (Shen, 2011, 2012). High pollutant reductions can be obtained by using a driveway protector mix, a commercial water-based TiO2 preparation, TiO2 in water, a water/cement slurry with low cement concentration, and the commercial PURETI coating. It was found that nitrogen oxide was efficiently removed with each of these treatments, while volatile organic compounds displayed more variability in removal efficiency. The infiltration rate reduction was largely influenced by different coating methods while none of the application methods decreased the infiltration rates below levels applicable for standard hydrological designs. Relative to traditional concrete, pervious concrete showed higher NO reductions.

3.1.2 Waste materials applications

Fly ash, as one of the most abundant waste materials in the world, has been introduced into general purpose Portland cement as a cementitious agent in pervious concrete samples. The properties of various pervious concretes containing fly ash (including density, porosity, compressive strength, water permeability and drying shrinkage) have been carefully measured (Aoki, 2012). Fly ash pervious concrete has the same trend of property variations as traditional pervious concrete. High porosity samples demonstrated higher permeability, whereas their compressive strength was reduced. It was found that there was no significant difference between properties of pervious concrete samples containing fly ash and those samples comprising only cement as a cementitious agent. Apart from the fly ash, the rice husk ash and fibers were used as cement replacement to prepare the pervious concrete. The mechanical properties testing results indicated that the rice husk ash has positive effects on the mechanical performance of the pervious concrete when combining with some fibers (Hesami, 2014). Another study compared five types of pozzolanic materials as cement replacement. It was found that replacement of 5% of the cement will lead to an enhancement of the compressive strengths and permeability of the high permeable concrete (Mohammed, 2013).

Li (2009) also claimed that a mixing design method for no-fines pervious recycled concrete or conventional pervious concrete is practical and feasible by using recycled aggregates. Some other wasted material, such as Washed municipal solid waste incinerator bottom ash (MSWIBA), was also used as substitute for natural aggregates in pervious concrete (Kuo, 2013). The mixture proportions, permeability, compressive strength, bending and split tensile strength were tested in this study. In specimens with the same water to cement ratio (W/C), the compressive, bending and split tensile strengths all increased with the ratio of filling paste. The connected porosity and permeability coefficients both decreased with increasing filling ratio.

Pervious concrete made with recycled concrete aggregate (RCA), which was obtained from decommissioned curbs and gutters, sidewalks, and parking lots, was prepared by substituting the coarse aggregate in the pervious concrete with 15%, 30%, 50%, and 100% RCA. The cylinders were cast in the laboratory for each percentage of RCA and a control mix containing only virgin aggregate. The compressive strength, permeability, and void content were tested (Rizvi 2010). It was found that the pervious concrete containing 15% RCA had similar strength, permeability, and void content to those of the control mix. Samples that contained 30% RCA or greater had a significant loss in strength and increase in permeability and void content. Similar results were demonstrated by Aamer Rafique Bhutta (2013). It was found that, if combined with Styrene butadiene rubber, the performance of the pervious concrete prepared with RCA will be acceptable.

Apart from the hard materials, soft materials were also used as aggregates to prepare the pervious concrete. Recently, rubber from waste tires was used as the aggregate to prepare the pervious concrete (Shen, 2013; and Gesoğlu, 2014). The mechanical properties were investigated and the corresponding hydraulic performance was tested as well. The results show that the use of waste tire rubber can significantly aggravate the mechanical properties and permeability; however, the toughness, damping capacitance, and ductility can be considerably increased (Gesoğlu, 2014).

Similarly, Gaedicke (2014) investigated the properties of cores and compacted cylinders with various types of aggregates and different percentages of cement replacement by slag. In this study, the cores were comprised of pea gravel, limestone, and recycled aggregates. Relative to the compacted cylinders with a same porosity and same unit weight, the cores have 20% less permeability and 17% lower compressive strength.

Geopolymer has been studied as a binding material for pervious concrete (Tawatchai, 2012). It was found that the mechanical properties of the pervious concrete can be satisfied by using geopolymer as the binder material. The relationships of the density-void content, compressive strength-density, and compressive strength-void content were derived and found to be similar to those of conventional pervious concrete.

3.1.3 Heat island effects mitigation

The heat island phenomenon has already become a large concern due a global urbanization trend. Recently, pervious concrete pavement has been studied as a solution to this problem. In Haselbach's study, temperature data from a site in Iowa and heat storage phenomena for various weather patterns were presented (Haselbach, 2010). The site contained both pervious concrete pavement with a solar reflectance index (SRI) of 14 and traditional concrete pavement with an SRI of 37. A high SRI (>29) has been accepted by LEED as one method to characterize a surface as a cool surface. Combined with the high internal surface area, rainfall will result in significantly more removal of stored heat from the pervious concrete system and reduce the thermal shock from impervious surface runoff.

Herb (2008) developed a simple model to predict the surface heat transfer processes on impervious and pervious land surfaces for both dry and wet weather periods. In this study, equations were developed to predict the magnitude of the irradiative, convective, conductive and evaporative heat fluxes on a dry or wet surface using standard climate data as inputs.

Recently, a study demonstrated that wet pervious pavements have relatively lower surface temperatures than the impermeable pavements. It was found that the peak cooling temperatures was about 15-35ºC of the pavement surface in the early afternoon of the summer season in California (Li, 2013a).

3.1.4 Noise reduction

U.S. and European concrete pavement noise reduction methods were evaluated by Cackler (2006). Sound absorption levels for pervious concrete pavements have been shown to increase with higher porosity levels. Quieter pervious concrete also results from smaller aggregate sizes.

Schaefer (2011) also reported the noise reduction effects of pervious concrete overlay in MnROAD Low Volume Road and reveal a remarkably quiet pavement. In this report, it was found that the traditional concrete noise levels range from around 100 to 110 decibels adjusted (dBA), while the pervious concrete range was between 96 and 98 in 2009 and 2010.

Tian (2014) investigated the noise reduction effect of the pervious concrete pavement from both laboratory and field tests. It was found that the aggregate sizes and the thickness of the pervious concrete have considerable effects on noise reduction. The 9.5 mm aggregates size had the highest acoustical absorption coefficient, and the 80 mm thickness had the optimum noise absorption. The field testing results showed that the noise can reduce by 4-8 dB after application of pervious concrete pavement.

3.2 Designing and Preparation

3.2.1 Mix design and preparation

Zaldo (2006) claimed that the durability of pervious concrete depends on three primary factors: mix design, placement, and proper maintenance. Wang (2006) and Putman (2011) studied mix proportion design and preparation techniques of pervious concrete and Schaefer *el.al*. (Schaefer, 2006) found saturated freeze-thaw performance (using ASTM C666) could be improved by several different changes to the mix design: using a small amount of fine aggregate (sand), adding polypropylene fibers, using a slightly higher water/cement ratio, increasing compaction (lower porosity), including entrained air and increasing paste volume, replacing some Portland cement with fly ash or silica fume, or using a latex admixture (Kevern, 2008b; Wu, 2010).

Kevern *et.al*.(2006, 2008a, 2008c, 2009a, 2009b, 2010b) also published many works on mixture proportion design and methods development, especially in cold weather climates (Kevern, 2005, 2008a, 2008b, 2008d, 2010a).

Deo (2011) developed a methodology to proportion pervious concrete mixtures of desired porosity using high or low cement paste contents. A consistent trend of decreasing peak stresses and strains at peak stress with increasing porosity was obtained. A reduction in strains at peak stresses with decreasing paste contents and a rapid drop in the post-peak response with decreasing porosity was also observed. The compressive energy absorbed by the pervious concrete specimens was found to scale linearly with compressive strength and was related to the porosity and critical pore sizes in the material.

3.2.2 Modeling and simulation

Deo (2010) used a statistical model to build a relationship between the compressive strength and the relevant pore structure features. This model was then used as a base model in a Monte-Carlo simulation to evaluate the sensitivity of the predicted compressive strength to the model terms. Lian also presented a discrete element numerical method by using particle flow code to evaluate the structural properties of porous concrete (Lian, 2011a, 2011b).

The condition index and performance models were developed to simulate the application of pervious concrete pavement under different conditions, especially in winter seasons, and were modeled by soft computing techniques (Fuzzy sets, Latin Hypercube Simulation technique, and Markov Chain process), Bayesian Statistical technique, and specific panel rating method and regression analysis techniques (Golroo, 2009, 2010, 2011, 2012a, 2012b, 2012c, 2012d).

Cofer *et.al* developed a finite element modeling procedure for pervious concrete pavement systems (Alam A, 2012). With an assumption of perfect bond between the interfaces of the different material layers, a simplified vertical porosity distribution in the previous concrete layer was used for the modeling procedure. All the modeling analyses were for static loading conditions and linear material properties. It was found that, if the pavement condition index data is defined to represent cyclic loading, the required thickness needs a factor of safety of approximately two relative to the static loading analysis. In addition, expanded finite element models for typical material properties and tire pressures indicate that pervious concrete might be appropriate for high volume traffic applications such as highway shoulders.

A statistical model was developed to investigate the effects of W/C, cement content and coarse aggregate content on the density, void ratio, infiltration rate, and compressive strength of Portland cement pervious concrete (Sonebi, 2013). It was found that the W/C, cement content, coarse aggregate content and their interactions are key parameters that significantly affect the characteristic performance of pervious concrete. The developed statistical models can facilitate optimizing the mixture proportions of pervious concrete for the final performance.

3.3 Properties Evaluation

3.3.1 Hydraulic and infiltration properties

Permeability tests are frequently conducted in the laboratory on pervious concrete samples. While not yet standardized by ASTM or AASHTO, the most common type of laboratory test is a falling head permeability test (McCain, 2010; Huang, 2010, Rizivi, 2010; and Schaefer, 2006). In this test type of test, a sample is sealed on the sides and the amount of time for water applied to the surface of the sample to drop in height is recorded. The time and beginning and ending pressure head are used to compute hydraulic conductivity. Two options for testing the infiltration rate in the field include ASTM C1701 and a method developed and refined over several years by Minnesota DOT personnel (personal communication with Bernard Izevbekhai, MnDOT).

Luck *et.al.* tested the hydraulic properties of pervious concrete in detail (Luck, 2006, 2008, 2009) and found pervious concrete has a great potential for mitigating negative impacts on the natural environment. In addition to the runoff reduction properties, it also provides obvious benefits relative to typical impervious concrete.

In a study by Chai, the hydraulic performance of fully permeable highway shoulder retrofits was designed to capture all the rainfall runoff falling onto conventional highway surface pavements (Chai, 2012). The authors claimed that an aggregate depth of about 1.5 m was adequate for most California areas with two-lane highways. Sensitivity analyses also revealed that the saturated hydraulic conductivity (Ks) of the subgrade soil is the most important parameter to be considered in the design of fully permeable pavements with a minimum effective allowable value of approximately 10^{-5} cm/s.

The hydraulic performance of pervious concrete pavements from field and laboratory settings was investigated to evaluate the infiltration capacities of pervious concrete cores, the underlying soils and the usefulness of rejuvenation methods in restoring their hydraulic performance (Chopra M, 2010). In this study, a new field test device called an embedded ring infiltrometer was developed for evaluating the infiltration rates of newly installed pervious concrete pavements. It was demonstrated that the rejuvenation methods can substantially restore the performance of pervious concrete pavements for better management of stormwater.

In fact, there is a strong relationship between the porosity and the hydraulic properties of pervious concrete (Montes, 2006). Increasing porosity has a positive influence on the hydraulic properties while it has a negative influence on the strengths. Huang (2010) and Shu (2011) studied the influence of porosity on the hydraulic properties and strengths. Latex polymer, sand, and fiber were used to improve the strength of pervious concretes of the same porosity without sacrifice to the hydraulic properties. They found that it was possible to produce a pervious concrete mixture with acceptable permeability and strength through the combination of latex and sand (Huang, 2010).

More recently, it has been recognized that the vertical porosity distribution is playing a key role on the hydraulic properties of pervious concrete (Martin III, 2014). However, the real impact of the vertical distribution on the hydraulic performance of the pervious concrete pavement is still not very clear, especially in a quantitative way. How to accurately characterize the vertical porosity is an important research topic that needs to be further investigated in future studies.

Of particular note, recent research has found that the hydraulic properties of pervious concrete are largely determined by the testing methods (Brown, 2014). By comparing the two most widely used methods, the National Center for Asphalt Technology (NCAT) permeameter and the ASTM C1701, it was found that the permeability measured by ASTM 1701 is about 50% to 90% lower than those measured by the NCAT approach (Li, 2013b).

3.3.2 Mechanical properties

The effects of aggregate gradation, amount and size on the static modulus of elasticity of pervious Portland cement concrete were evaluated using four different mixtures (Crouch, 2007). It was reported that for a uniform gradation, the compressive strength and static elastic moduli appeared to be higher within an optimal range of voids. An increased aggregate amount resulted in a statistically significant decrease in both compressive strength and static elastic moduli. While the compressive strengths were higher for mixtures containing smaller aggregate sizes, there was no significant difference between the static elastic moduli when different aggregate sizes were used.

Deo (2010) studied the material structure-compressive response relationships in pervious concretes. They found that compressive strengths increased with increasing aggregate size and paste volume fractions. Meanwhile, the compressive response was influenced by the size, distribution and spacing of pores.

Structural performance of pervious pavements was investigated by Geode *et.al.* Distress surveys were performed on two field installations of pervious concrete which were subjected to equivalent traffic stresses as some collector streets that had been in use for 20 years (Geode, 2012). The high pavement condition index ratings of the thicker pervious concrete sections indicate that pervious concrete, when properly designed, is capable of being used for many collector streets and most residential streets for 20-30 years while exhibiting structural performance similar to traditional pavements. Even though the pervious concrete analyzed was subjected to an equivalent amount of stress from loading as a collector street in use for between 8 and 80 years, it was only subjected to weathering stresses during its actual life. In addition, the mechanical performance and structural integrity of the pervious concrete pavements were evaluated most recently. It was claimed that the deflection of the pervious concrete pavements is largely affected by the subbase materials and the compaction of the layers. The deflection of the pervious concrete pavement with a loading application was about 1.7 to 4 times higher than the impervious concrete pavement which is determined by the subbase characterization (Gogo-Abite, 2013).

In Chen's study (Chen, 2012), pervious cement concrete samples modified with either polymers or supplementary cementitious materials (SCM) were analyzed for fatigue properties, fracture energies and compressive and flexural strengths. It was found that the strength development of SCM modified pervious concrete was different from the polymer-modified pervious concrete. Polymer modified pervious concrete has higher flexural strength and remarkably higher flexural-to-compressive strength ratio than SCM modified pervious concrete at the same porosity level. Polymer modified pervious concrete displays far longer fatigue life than SCM modified pervious concrete for any given failure probability and at any stress level. Porosity had little effect on the strength development of either modified concrete.

The damping properties of pervious concrete with water, glycerol, and glycerol/water blends constituting the pore fluid at loading frequencies ranging from 0.01–25 Hz was studied by Leung (2012). It was claimed that a significant poromechanical damping can be generated and that the frequency at which the damping is maximized can be controlled by changing material properties. It was also discovered that poromechanical modeling underpredicts the measured damping increase resulting from the saturation status.

Stiffness and fatigue were analyzed by means of Westergaard's theory of a medium-thick plate on a Winkler foundation (Vancura 2011b). The stiffness evaluation compared the responses of pervious and conventional concrete pavements to falling weight deflectometer stresses and to models created in

ISLAB2005. Additionally, a fatigue analysis of pervious concrete was completed through use of the StreetPave fatigue model.

The fracture toughness of pervious concrete was studied by Rehder (2014). It was found that the fracture toughness was largely determined by the porosity of the pervious concrete. However, if the porosity is similar, the fracture toughness will be governed by the pore sizes. Increasing the pore size will considerably reduce the fracture toughness of the pervious concrete.

3.3.3 Abrasion resistance and skid resistance

The abrasion resistance of pervious concrete can be easily measured following ASTM C1747 using a Los Angeles abrasion machine with parameters specifically developed for pervious concrete. Wu (2010) found adding styrene butadiene rubber (SBR) latex polymer to pervious concrete mixes significantly improved abrasion resistance, and, although it decreased, had adequate permeability.

Pervious concrete pavements are reported to have improved skid resistance (McCain, 2010; Izevbekhei, 2008; Schaefer, 2011), although little supporting data was found in a cursory search of literature. Tests in a Pennsylvania parking lot with pervious concrete using a British pendulum tester (ASTM E303) showed pervious concrete had similar skid resistance to traditional asphalt and porous asphalt (Houle, 2008). The properties of pervious concrete and porous asphalt were also compared side-by-side (Welker, 2012).

3.4 Durability and Maintenance

3.4.1 Freeze-thaw in cold weather

Yang (2011) found silica fume, polypropylene fibers, and/or increased cement content also improved saturated freeze–thaw durability, particularly for water-cured specimens. Unclogged, unsaturated pervious concrete specimens tested for freeze–thaw resistance with ASTM C666 had significantly greater durability than either clogged and/or saturated specimens with no significant differences in structural properties (Guthrie, 2010).

McCain *et.al.* (2006) in Vermont found during a laboratory study that a large application of a sand-salt mixture (2:1 by weight) at 0.24 lb/ft^2 (equivalent to 15,200 lb/lane·mile) reduced the hydraulic conductivity of laboratory-mixed pervious concrete specimens by about 15 percent. Adding sand to the surface and shaking the samples simulated maximum clogging and reduced the hydraulic conductivity by about 35 percent. Vacuuming the samples restored the hydraulic conductivity to approximately 90 percent of their initial values.

According to the EPA, traction sand should not be applied to pervious concrete pavements. Also, because pervious concrete does not treat chloride or other deicers, reduced application rates of deicers are needed (Environmental Protection Agency). Several pervious concrete sections were constructed at

MnROAD (a Minnesota DOT pavement research facility) between 2006 and 2008 and have not been impacted by any sanding, salting, or plowing operations (personal communication with Bernard Izevbekhai, MnDOT). Thus, research is needed to ensure pervious concrete installed by NDOT will be durable and effective under their normal winter maintenance operations.

Pervious concrete pavement cores removed from the field were investigated in the laboratory. (Delatte N, 2009, Henderson, 2009). Generally speaking, the pervious concrete pavement performed well in freeze-thaw environments with little maintenance required after installation. No visual indicators of freeze-thaw damage were observed. With the exception of some installations in which the pore structure was sealed during construction with wet mixtures or over compaction, nearly all sites showed fair to good infiltration capability based on drain-time measurements.

Culter *et.al.* developed two concrete mixes (with and without latex modification) and subjected them to three deicing chemicals (sodium chloride, calcium chloride, and calcium-magnesium acetate), under a freezing–thawing or drying–wetting condition. Meanwhile, two deicing chemical application methods (saturated and drained) were employed (Culter 2010). It was observed that the calcium chloride solution caused the most damage, while the calcium magnesium acetate caused the least. The saturated scaling test method, followed according to ASTM C672, provided much higher mass loss of tested concrete samples when compared with a modified, more realistic drained test method. Both the saturated and drained test results indicated that wet cured pervious concrete with latex polymer had much higher mass loss than the one without latex polymer, regardless of the type of deicing chemicals.

Guthrie (2010) evaluated the resistance of pervious concrete to degradation during freeze–thaw cycling under different soil clogging and water saturation conditions. In this study, both soil clogging and water saturation reduced the freeze–thaw durability of pervious concrete. Specimens that remained unclogged and unsaturated were damaged at a significantly faster rate than those specimens that were clogged with soil, completely submerged in water, or both. A comparison of in situ modulus values, core modulus values and core compressive strengths associated with clogged and unclogged locations in the experimental pervious concrete slab indicated no significant differences in structural properties in the clogged and unclogged locations. Only the upper 1 to 2 inches of pervious concrete in clogged locations were filled with soil; the remaining depth of the slab appeared to be free draining.

The pervious concrete performance and the maintenance methods of five field sites in Canada have been studied (Henderson, 2011 and 2012). The testing involved surface distress evaluations, permeability monitoring and evaluation of cast and cored samples. Winter and rehabilitative maintenance options were performed and evaluated. The results indicate that the freeze–thaw cycles were not the main reason for distress development or failure. The factors of greater concern are the site design, mix design and construction stages. The maintenance methods used were broom or street sweeping, rinsing the surface with a garden hose or large hose, vacuuming and power washing.

3.4.2 Clogging

Recently, clogging problems have piqued the interests of many researchers (Sriravindrarajah 2011; Sansalone 2012; Wang, 2012; Vancura, 2012). A “clogging potential” was defined (Deo, 2010) as either a ratio of the porosity reduction because of clogging to the initial porosity, or as a ratio of the permeability reduction to the permeability in the unclogged state. The influence of pore structure features on particle retention and the consequent permeability reduction were systematically investigated using several pervious concrete mixture proportions with different size aggregates (Deo, 2010). Significant permeability reductions were observed when finer sand was used as the clogging material. Pervious concrete specimens of similar porosity having very large (5–6 mm) or very small (1–2 mm) pore sizes were found to be less susceptible to clogging.

Pervious concrete facing a series of catastrophic clogging cycles with clay laden runoff was presented in a laboratory procedure (Haselbach, 2010). In this study, the clay materials were assumed to remain near the surface of pervious concrete systems, since most placements have a vertical porosity distribution with the smaller pores near the top. By testing core samples from actual field placement, the experimental results show that substantial deposition of clay on a pervious concrete pavement will largely reduce its service capability, even when fully “clogging” the pavement only temporarily. Despite the clay remains at the surface, the infiltration capacity of the pervious concrete was acceptable with simple maintenance such as surface sweeping and subsequent rinsing similar to rainfall events. Sriravindrarajah has done similar research on the influence of clay on the clogging phenomena of pervious concrete (Sriravindrarajah, 2011).

In addition to the clay clogging testing, by combining with experimental results, a theoretical relation was also developed to predict the relationship between the effective permeability of a sand-clogged pervious concrete block, the permeability of sand, and the porosity of the unclogged block (Haselbach, 2006). The experimental results agreed well with the theoretical calculated permeability of the pervious concrete system for pervious concrete systems fully covered on the surface with sand. In this study, a typical pervious concrete block will allow water to pass through at flow rates greater than 0.2 cm/s and a typical extra fine sand will have a permeability of approximately 0.02 cm/s. The limit of the system with complete sand coverage resulted in an effective system permeability of approximately 0.004 cm/s, which is similar to the rainfall intensity of 30 min duration.

The clogging dynamics of pervious concrete were assessed with time domain reflectometers in Edison, New Jersey, and Louisville, Kentucky (Brown, 2013). In this study, the paired time domain reflectrometers were installed at two locations at the depth of 0.4 meter below the driving surface. The placement strategy of the time domain reflectometers was used to evaluate the spatial infiltration of runoff and to record the clogging and infiltration dynamics. It was found that the clogging was developed from the upgradient edge, and the Lousiville case study can support the potential surface clogging mechanism.

Based on the clogging problem, some maintenance methods were developed to clean the pervious concrete pavements, including power blowing, pressure washing, and vacuuming, or the combination of these methods. It was found that pressure washing and vacuuming are both effective to clean the clogging. They can increase the infiltration rate by over 90%. The cleaning effect will be considerably increased by combining use of these methods (Hein, 2013).

A quick surface infiltration test was presented for assessment of pervious concrete maintenance needs (Dougherty, 2011). Pressure washing and pressure washing with power blowing were applied. Both maintenance practices improved the pervious concrete sidewalk infiltration rates by 20-fold on average. If combined with pressure washing and power blowing, an almost 200-fold increase can be observed on sites.

A laboratory study was performed to measure clogging by sand and clay in a saturated pervious concrete pavement system and the subsequent effect of surface cleaning by pressure washing (Coughlin, 2012). Researchers found that measurable clogging caused by both sand and clay could not be reversed by pressure washing. However, even after clogging, the infiltration and exfiltration rates were well above the average intensity for the 100-year 1-h design storm, but its performance for storm-water infiltration will be limited by the rate of exfiltration to the subgrade.

The stormwater management, infiltration rates, rejuvenation techniques, sustainable storage of the components and complete systems, water quality and strength properties of pervious concrete pavements were investigated in Chopra's study (Chopra, 2007 and 2011). The use of a vacuum sweeper truck was ineffective at removal of deep penetrating clogging, although it can successfully remove surface sediments. The reduction in infiltration rates is only observed when significant amounts of sediments enter the system and migrate into deeper locations.

3.5 Characterization

The internal structure, including the size, shape and distribution of the pores and aggregates, is the key factor in determining the final properties of pervious concrete. By using 3D CT images (shown as Figure 3.3), the relationship between the internal structures and the final properties of the pervious concrete was analyzed (Kayhanian 2012). It was found that the scanned image analysis showed that most clogging occurs near the surface of the pavement. While lower porosity generally appeared to be limited to the upper 25 mm, in some core samples evidence of lower porosity was found up to 100 mm below the surface. A recent study by Manahiloh found similar results (Manahiloh, 2012).

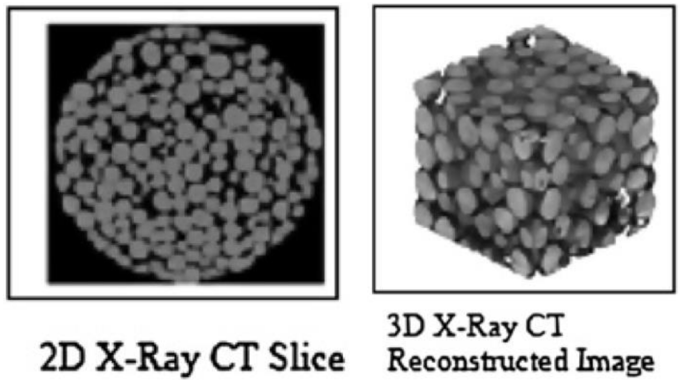

Fig. 3. 3 X-ray 2D and 3D flash CT images of pervious concrete materials (Kayhanian 2012)

The entrained air voids in pervious concrete were characterized according to ASTM C457 using a RapidAir system. The compressive strength, tensile strength, and freeze-thaw durability (ASTM C666A) of the pervious concrete were tested (Kevern, 2008d). Figure 3.4 shows the images of typical pervious concrete samples prepared with limestone with no air entraining agent and limestone with double synthetic air entraining agent. According to the microstructure analysis, by using an air entrainment agent the workability of pervious concrete will be improved and thus reduces the overall porosity and increases the unit weight of the pervious concrete. The strength and freeze-thaw durability also increases with the level of entrained air in pervious concrete.

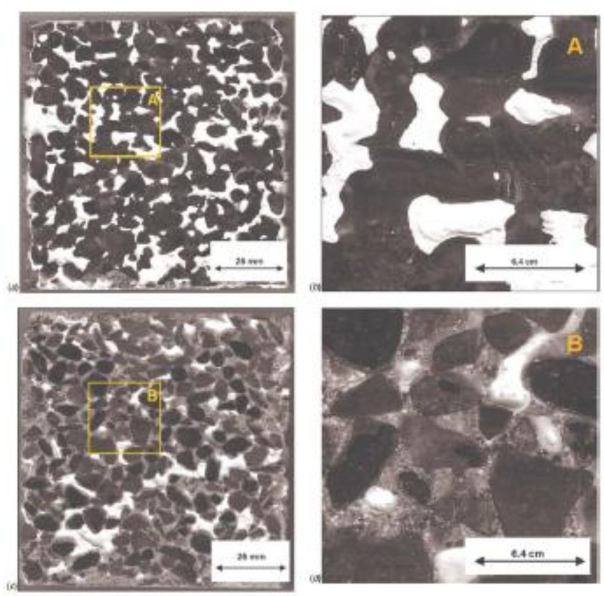

Fig. 3. 4 Images of typical pervious concrete samples. (a) Limestone with no air entraining agent, (b) Limestone with double synthetic air entraining agent, (c) Area A in (a). (d) Area B in (b). (Kevern, 2008d)

The porosity and physical features of the pore network were characterized (Neithalath 2007) by using Electrical Impedance Spectroscopy (EIS) incorporating a modified version of Archie's law. The pore volume, sizes, and connectivity in pervious concretes were characterized for permeability testing (Neithalath 2010). The Weibull probability distribution function was found to describe the pore size distribution in pervious concretes. By using an electrical conductivity ratio along with the pore phase connectivity, the values of porosity and pore sizes that were determined by morphologies (shown as Figure 3.5) were used in a Katz-Thompson type relationship to predict the permeability of pervious concretes.

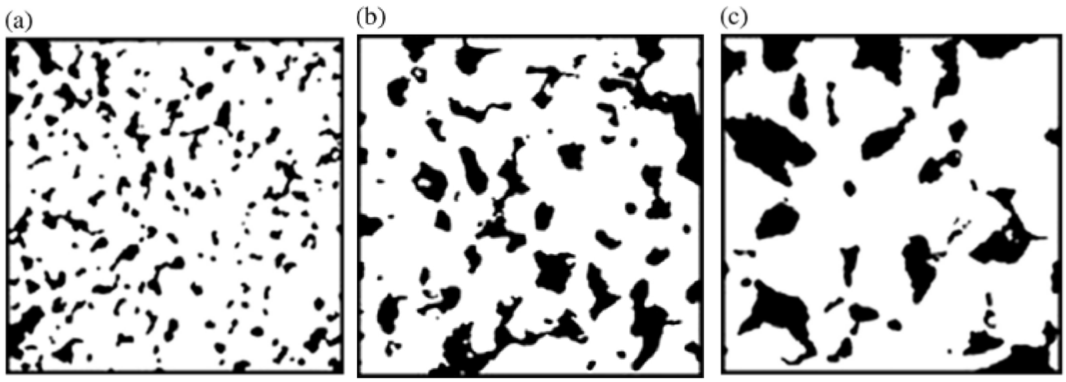

Fig. 3. 5 Two-dimensional images of planar sections from pervious concrete mixture proportions with (a) 2.36 mm, (b) 4.75 mm, and (c) 9.5mm maximum size aggregates (Neithalath 2010a and 2010b)

Sumanasooriya (2009, 2011, 2012) also characterized the pore structure reconstruction of three-dimensional material structures of pervious concretes using two-dimensional digital images obtained from actual specimens. She also used computational permeability predictions using these reconstructed three-dimensional material structures to predict the final properties of the pervious concrete, as shown in Figure 3.6.

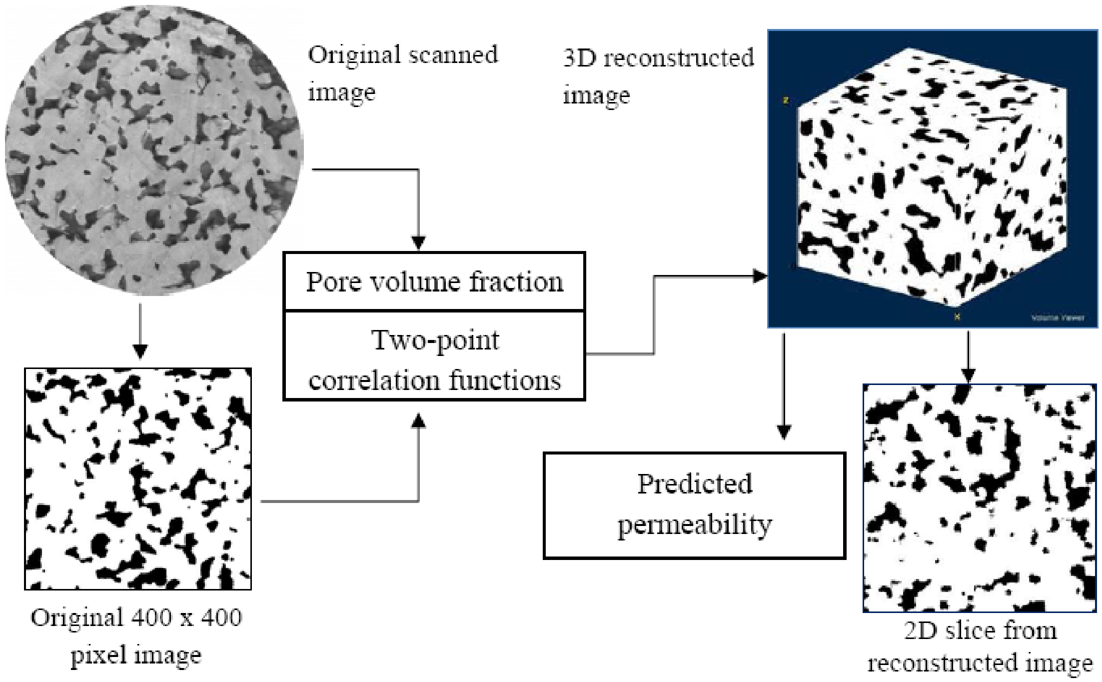

Fig. 3. 6 Steps involved in 3D reconstruction and permeability prediction

The paste and aggregate distresses and the crack propagation in pervious concrete in a wet, hard freeze climate were investigated by microscopic analysis (Vancura 2011a). Figure 3.7 shows the morphologies of the pervious concrete demonstrating the crack propagation and the interfacial transition zone (ITZ) areas.

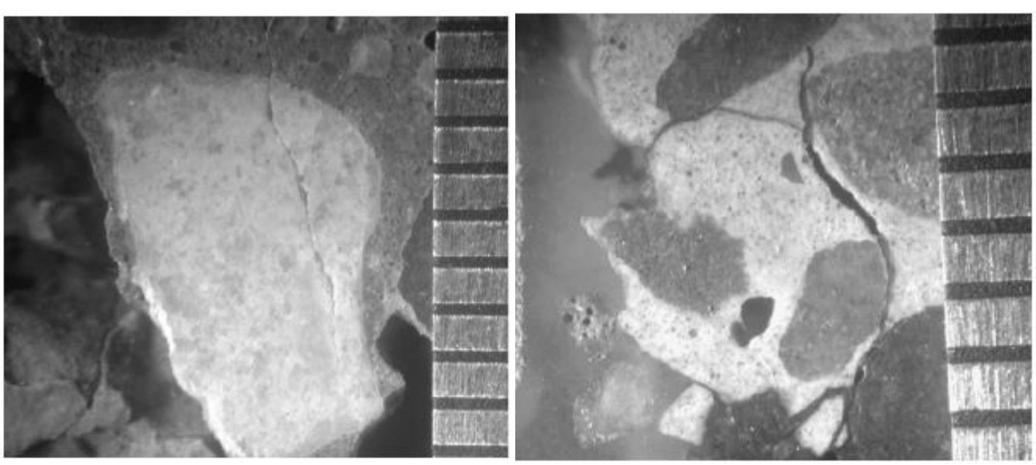

Fig. 3. 7 The morphologies of pervious concrete demonstrating the cracks propagation and the ITZ areas (Vancura 2011a).

3.6 Concluding remarks and future study trends

- Pervious concrete has been increasingly used as a powerful tool for low impact development. It has many environmental advantages for urban cities, including stormwater runoff management, traffic noise control, groundwater recharge, and mitigation of the urban heat island.
- The various mixes proportions can produce a wide range of properties in pervious concrete pavement, and various additives are helpful to enhance the overall performance of pervious concrete materials.
- In general, it is hard to optimize the mechanical properties and the infiltration performance of pervious concrete at the same time. New technologies need to be developed to help increase the mechanical properties without significantly sacrificing the infiltration properties.
- Freeze/thaw damage, deicer impacts, and clogging phenomenon still create bottleneck problems for the implementation of pervious concrete pavements.
- Ongoing challenges include quantitatively characterizing pervious concrete materials and establishing the quantitative relationship between the pore structure and the performance of pervious concrete.

3.7 References

Aamer, Rafique, Bhutta, M., Hasanah, N., Farhayu, N., Hussin, M. W., Tahir, M. B. M., and Mirza, J. 2013. Properties of porous concrete from waste crushed concrete (recycled aggregate). Construction and building materials, 47, 1243-1248.

Alam, A., Haselbach L., Cofer, W., 2012, Finite Element Evaluation of Pervious Concrete Pavement for Roadway Shoulders. A final report prepared for the United States Department of Transportation.

Aoki, Y, Ravindrarajah, R.S, and Khabbaz, H, 2012, Properties of Pervious Concrete Containing Fly Ash. Road Materials and Pavement Design, 13(1), 1-11.

Bedan, E. S. and Clausen JC, 2009, Stormwater Runoff Quality and Quantity from Traditional and Low Impact Development Watersheds, Journal of the American Water Resources Association, 45(4), 998-1008.

Brown, H.J. Monitoring Pervious Concrete for Water Quality in a Laboratory and Field Environment. Presented online : http://www.rmc-foundation.org/images/PCRC%20Files/Hydrological%20&%20Environmental%20Design/Monitoring%20Pervious%20Concrete%20for%20Water%20Quality%20in%20a%20Laboratory%20and%20Field%20Environment.pdf

Brown, R. A., and Borst, Michael. 2013, Assessment of Clogging Dynamics in Permeable Pavement Systems with Time Domain Reflectometers. Journal of Environmental Engineering 139, no. 10, 1255-1265.

Brown, R. A., & Borst, M. 2014. Evaluation of Surface Infiltration Testing Procedures in Permeable Pavement Systems. Journal of Environmental Engineering, 140(3).

Bury, M. A., Mawby C. A., and Fisher D. Making Pervious Concrete Placement Easy Using a Novel Admixture System. Presented online : http://www.rmc-foundation.org/images/PCRC%20Files/Mix%20Design/Making%20Pervious%20Concrete%20Placement%20Easy%20Using%20a%20Novel%20Admixture%20System.pdf

Brown H. J., Monitoring Pervious Concrete for Water Quality in a Laboratory and Field Environment, Presentation, online, http://www.rmc-foundation.org/images/PCRC%20Files/Hydrological%20&%20Environmental%20Design/Monitoring%20Pervious%20Concrete%20for%20Water%20Quality%20in%20a%20Laboratory%20and%20Field%20Environment.pdf

Brown, R. A., Line, D.C., and Hunt, W.F., 2012, LID Treatment Train: Pervious Concrete with Subsurface Storage in Series with Bioretention and Care with Seasonal High Water Tables. Journal of Environmental Engineering. 2012.138, 689-697.

Cackler, E. T., Ferragut, T., Harrington, D. S., Rasmussen, R. O., and Wiegand, P, 2006, Evaluation of U.S. and European Concrete Pavement Noise Reduction Methods, technical report prepared for the Federal Highway Administration under Cooperative Agreement DTFH61-01-X-00042.

Chai, L., Kayhanian, M., Givens, B., Harvey, J.T., and Jones, D. 2012, Hydraulic Performance of Fully Permeable Highway Shoulder for Storm Water Runoff Management. Journal of Environmental Engineering. 138, 711-722.

Chen, Y., Wang, K. J., Liang, D., 2012, Mechanical properties of pervious cement concrete, Journal of Central South University, 19, 3329-3334.

Chopra, M., Wanielista, M., Ballock, C., Spence, J., 2007, Construction and Maintenance Assessment of Pervious Concrete Pavements, A final report prepared for the Florida Department of Transportation, Orlando, FL.

Chopra, M., Hardin, M., and Wanielista, M., 2011, Pervious Pavements-Installation, Operations and Strength, a final report prepared for the Florida Department of Transportation.

Chopra, M., Kakuturu, S., Ballock, C., Spence, J., and Wanielista, M., 2010. Effect of Rejuvenation Methods on the Infiltration Rates of Pervious Concrete Pavements. Journal of Hydrologic Engineering, Jun. 426-433.

Coughlin, J.P., Campbell, C.D.; and Mays, D.C., 2012, Infiltration and Clogging by Sand and Clay in a Pervious Concrete Pavement System. Journal of Hydrologic Engineering, 17, 68-73.

Crouch, L.K., Smith, N., Walker, A.C., Dunn, T.R., and Sparkman, A. Determining Pervious PCC Permeability with a Simple Triaxial Flexible-Wall Constant Head Permeameter. Presented online : http://www.rmc-foundation.org/images/PCRC%20Files/Specifications%20&%20Test%20Methods/Determining

%20Pervious%20PCC%20Permeability%20with%20a%20Simple%20Triaxial%20Flexible-Wall%20Constant%20Head%20Permeameter.pdf

Crouch, L.K, Smith, N., Walker, A.C., Dunn, T.R., and Sparkman, A. Pervious PCC Compressive Strength in the Laboratory and the Field: The Effects of Aggregate Properties and Compactive Effort. Presented online : http://www.rmc-foundation.org/images/PCRC%20Files/Construction%20Techniques/Pervious%20PCC%20Compressive%20Strength%20in%20the%20Laboratory%20and%20the%20Field.pdf

Crouch, L.K., Pitt, J.; and Hewitt, R., 2007, Aggregate Effects on Pervious Portland Cement Concrete Static Modulus of Elasticity. Journal of Materials in Civil Engineering. Jul. 2007, pp. 561-568.

Cutler HE, Wang KJ, Schaefer VR, and Kevern JT, 2010, Resistance of Portland Cement Pervious Concrete to Deicing Chemicals, Transportation Research Record: Journal of the Transportation Research Board, No. 2164, Transportation Research Board of the National Academies, Washington, D.C., pp. 98–104.

Deo O, Sumanasooriya M, and Neithalath N., 2010, Permeability Reduction in Pervious Concretes due to Clogging: Experiments and Modeling, Journal of Materials in Civil Engineering, Jul. 741-751

Deo O, Neithalath N, 2010, Compressive Behavior of Pervious Concretes and a Quantification of the Influence of Random Pore Structure Features. Materials Science and Engineering A., 528, 402-412.

Deo O, Neithalath N, 2011, Compressive Response of Pervious Concretes Proportioned for Desired Porosities. Construction and Building Materials, 25, 4181-4189.

Delatte N, Mrkajic A, and Miller DI., 2009, Field and Laboratory Evaluation of Pervious Concrete Pavements. Transportation Research Record: Journal of the Transportation Research Board, No. 2113, Transportation Research Board of the National Academies, Washington, D.C., pp. 132–139.

Dougherty M, Hein M, Martina BA, and Ferguson BK, 2011, Quick Surface Infiltration Test to Assess Maintenance Needs on Small Pervious Concrete Sites. Journal of Irrigation and Drainage Engineering, 137, 553-563.

Earles TA, WRE D, Keyes J, and Claffey M, 2008, Monitoring of Pervious Pavement/Infiltration Bed System in Aurora, Colorado, World Environmental and Water Resources Congress. Ahupua'a.

Environmental Protection Agency, NPDES, Stormwater BMPs, Pervious Concrete Pavement website: http://cfpub.epa.gov/npdes/stormwater/menuofbmps/index.cfm?action=browse&Rbutton=detail&bmp=137&minmeasure=5

Gaedicke, Cristián, Armando Marines, and Farel Miankodila. 2014, A method for comparing cores and cast cylinders in virgin and recycled aggregate pervious concrete. Construction and Building Materials 52, 494-503.

Garber S, Rasmussen RO, and Harrington D, 2011, Guide to Cement-Based Integrated Pavement Solutions, Technical report prepared for the Portland Cement Association.

Gesoğlu, M., Güneyisi, E., Khoshnaw, G., and İpek, S. 2014. Investigating properties of pervious concretes containing waste tire rubbers. Construction and Building Materials, 63, 206-213.

Goede W and Haselbach L, 2012, Investigation into the Structural Performance of Pervious Concrete. Journal of Transportation Engineering, 138, 98-104.

Gogo-Abite, I., Chopra, M., & Uju, I. 2013. Evaluation of Mechanical Properties and Structural Integrity for Pervious Concrete Pavement Systems. Journal of Materials in Civil Engineering, 26(6).

Golroo A and Tighe SL. 2009, Use of Soft Computing Applications to Model Pervious Concrete Pavement Condition in Cold Climates, Journal of Transportation Engineering, 135,791-800.

Golroo A and Tighe SL. 2010, Developing an Overall Combined Condition Index for Pervious Concrete Pavements Using a Specific Panel Rating Method. Transportation Research Record: Journal of the Transportation Research Board, No. 2153, Transportation Research Board of the National Academies, Washington, D.C., 2010, pp. 40-48.

Golroo A, Tighe SL, 2011, Alternative modeling framework for pervious concrete pavement condition analysis. Construction and Building Materials, 25, 4043-4051.

Golroo A. and Tighe SL., 2012a, Development of Panel Rating Protocol and Condition Evaluation Model for Pervious Concrete Pavement, Journal of Transportation Engineering . 138, 634-648.

Golroo A. and Tighe SL., 2012b, Pervious Concrete Pavement Performance Modeling Using the Bayesian Statistical Technique. Journal of Transportation Engineering, 138, 603-609.

Golroo A. and Tighe SL., 2012c, Development of Pervious Concrete Pavement Performance Models Using Expert Opinions. Journal of Transportation Engineering, 138, 634-648.

Golroo A. and Tighe SL., 2012d, Pervious Concrete Pavement Performance Modeling: an Empirical Approach in Cold Climates, Canadian Journal of Civil Engineering, 39, 1100-1112.

Guthrie WS, DeMille CB, and Eggett DL. 2010, Effects of Soil Clogging and Water Saturation on Freeze–Thaw Durability of Pervious Concrete. Transportation Research Record: Journal of the Transportation Research Board, No.2164, Transportation Research Board of the National Academies, Washington, D.C., 2010, pp. 89–97.

Haselbach L., Poor, C., & Tilson, J. 2014. Dissolved zinc and copper retention from stormwater runoff in ordinary portland cement pervious concrete. Construction and Building Materials, 53, 652-657.

Haselbach L, Valavala S, Montes F., 2006, Permeability Predictions for Sand-Clogged Portland Cement Pervious Concrete Pavement Systems. Journal of Environmental Management, 81, 42-49.

Haselbach L, 2010, Potential for Clay Clogging of Pervious Concrete under Extreme Conditions, Journal of Hydrologic Engineering, 15, 67-69.

Haselbach L, Boyer M, Kevern JT, and Schaefer VR. 2011, Cyclic Heat Island Impacts in Traditional versus Pervious Concrete Pavement Systems. TRB 2011 Annual Meeting.

Hein MF, Dougherty, M., & Hobbs, T. 2013. Cleaning Methods for Pervious Concrete Pavements. International Journal of Construction Education and Research, 9(2), 102-116.

Henderson V, Tighe S, and Norris J, 2009, Pervious Concrete Pavement-Integrated Laboratory and Field Study. Transportation Research Record: Journal of the Transportation Research Board, No. 2113, Transportation Research Board of the National Academies, Washington, D.C., pp. 13-21.

Henderson V. and Tighe S., 2011, Evaluation of pervious concrete pavement permeability renewal maintenance methods at field sites in Canada. Canadian Journal of Civil Engineering. 38, 1404-1413.

Henderson V. and Tighe S., 2012, Evaluation of Pervious Concrete Pavement Performance in Cold Weather Climates. International Journal of Pavement Engineering. 13(3), 197-208.

Herb WR, Janke B, Mohseni O, Stefan HG., 2008, Ground surface temperature simulation for different land covers. Journal of Hydrology, 356, 327-343.

Hesami, S., Ahmadi, S., and Nematzadeh, M. 2014. Effects of rice husk ash and fiber on mechanical properties of pervious concrete pavement. Construction and Building Materials, 53, 680-691.

Houle KM, 2008, Winter Performance Assessment of Permeable Pavements: A comparative study of porous asphalt, pervious concrete, and conventional asphalt in a northern climate. M.S. Thesis, University of New Hampshire.

Huang BS, Wu H, Shu X, Burdette EG. 2010, Laboratory Evaluation of Permeability and Strength of Polymer-Modified Pervious Concrete. Construction and Building Materials, 24, 818-823.

Izevbekhei B, 2008, Pervious Concrete, TERRA Fact Sheet, November 2008.

Joung Y, Grasley ZC. 2008, Evaluation and Optimization of Durable Pervious Concrete for Use in Urban Areas. Research Report SWUTC/08/167163-1.

Kayhanian M, Anderson D, Harvey JT, Jones D, Muhunthan B., 2012, Permeability Measurement and Scan Imaging to Assess Clogging of Pervious Concrete Pavements in Parking Lots. Journal of Environmental Management, 95, 114-123.

Kevern JT, Wang K, Suleiman MT, and Schaefer VR, 2005, Mix Design Development for Pervious Concrete in Cold Weather Climates. Proceedings of the 2005 Mid-Continent Transportation Research Symposium, Ames, Iowa, August 2005.

Kevern JT, Wang K, Suleiman MT, and Schaefer VR, 2006, Pervious Concrete Construction: Methods and Quality Control. NRMCA Concrete Technology Forum: Focus on Pervious Concrete, May 24-25, Nashville, TN.

Kevern JT, Schaefer VR, Wang K, and Suleiman MT, 2008a, Pervious Concrete Mixture Proportions for Improved Freeze-Thaw Durability. Journal of ASTM International, 5(2), Paper ID JAI101320

Kevern JT, Wang K, and Schaefer VR, 2008b, Pervious Concrete in Severe Exposures- Development of pollution-reducing pavement for northern cities. Concrete international, July, 2008, 43-49.

Kevern JT, Wang K, and Schaefer VR, 2008c, Self-Consolidating Pervious Concrete. The Third North American Conference on the Design and Use of Self-Consolidating Concrete (SCC08).

Kevern JT, Wang K, and Schaefer VR, 2008d, A Novel Approach to Characterize Entrained Air Content in Pervious Concrete. Journal of ASTM International, 5(2), Paper ID JAI101434.

Kevern JT, Schaefer VR, and Wang K, 2009a, Predicting Performance of Pervious Concrete using Fresh Unit Weight. NRMCA Concrete Technology Forum: Focus on Performance Prediction, May 13-15.

Kevern JT, Schaefer VR, and Wang K, 2009b, Evaluation of Pervious Concrete Workability Using Gyratory Compaction. Journal of Materials in Civil Engineering. Dec. 764-770

Kevern JT, Schaefer VR, and Wang K, 2009c, Temperature Behavior of Pervious Concrete Systems, Transportation Research Record: Journal of the Transportation Research Board, No. 2098, Transportation Research Board of the National Academies, Washington, D.C., pp. 94–101.

Kevern JT, Wang K, and Schaefer VR, 2010a, Effect of Coarse Aggregate on the Freeze-Thaw Durability of Pervious Concrete. Journal of Materials In Civil Engineering . May. 469-475.

Kevern JT, 2010b, Evolution of Portland cement pervious concrete construction. Challenges, Opportunities and Solutions in Structural Engineering, and Construction – Ghafoori (ed.), 471-478.

Kevern JT, 2011, Operation and Maintenance of Pervious Concrete Pavements. TRB Annual Meeting. 11-0656.

Kwiatkowski M, Welker AL, Traver RG, Vanacore M, and Ladd T. 2007, Evaluation of an Infiltration Best Management Practice Utilizing Pervious Concrete. Journal of the American Water Resources Association. 43(5), 1208-1222.

Kuo WT, Liu CC, Su DS, 2013, Use of Washed Municipal Solid Waste Incinerator Bottom Ash in Pervious Concrete, Cement and Concrete Composites, DOI: http://dx.doi.org/10.1016/j.cemconcomp.2013.01.001

Lee MG., Chiu CT, Kan YC, Yen T. 2009, Experimental Study of Pervious Concrete on Parking Lot. GeoHunan International Conference. 125-131.

Leung CK, and Grasley ZC, 2012, Poromechanical Damping of Cementitious Materials. Journal of Materials in Civil Engineering, 24, 232-238.

Lian C, Zhuge Y. and Beecham S. 2011a, Modelling Pervious Concrete under Compression Loading - A Discrete Element Approach. Advanced Materials Research, 168-170, pp. 1590-1600.

Lian C, Zhuge Y. and Beecham S. 2011b, Numerical Simulation of the Mechanical Behavior of Porous Concrete. Engineering Computations: International Journal for Computer-Aided Engineering and Software, 28(8), pp. 984-1002.

Li H., Harvey JT, Holland TJ, and Kayhanian M. 2013a, The use of reflective and permeable pavements as a potential practice for heat island mitigation and stormwater management. Environmental Research Letters 8, 015023.

Li H., Kayhanian, M., & Harvey, J. T. 2013b. Comparative field permeability measurement of permeable pavements using ASTM C1701 and NCAT permeameter methods. Journal of environmental management, 118, 144-152.

Li H., Harvey J., and Ge Z. 2014. Experimental investigation on evaporation rate for enhancing evaporative cooling effect of permeable pavement materials. Construction and Building Materials, 65, 367-375.

Li JS, 2009, Mix Design of Pervious Recycled Concrete. GeoHunan International Conference, 103-108.

Luck JD, Workman SR, Higgins SF. and Coyne MS., 2006, Hydrologic Properties of Pervious Concrete. Transactions of the ASABE. 49(6), 1807-1813.

Luck JD, Workman SR, Coyne MS, Higgins SF., 2008, Solid Material Retention and Nutrient Reduction Properties of Pervious Concrete Mixtures, Biosystems Engineering. 100, 401-408.

Luck JD, Workman SR, Coyne MS, Higgins SF., 2009, Consequences of Manure Filtration through Pervious Concrete during Simulated Rainfall Events. Biosystems Engineering. 102, 417-423.

Manahiloh KN, Muhunthan B, Kayhanian M, and Gebremariam SY, 2012, X-Ray Computed Tomography and Nondestructive Evaluation of Clogging in Porous Concrete Field Samples.

Martin III, W. D., Kaye, N. B., & Putman, B. J. 2014. Impact of vertical porosity distribution on the permeability of pervious concrete. Construction and Building Materials, 59, 78-84.

Mbanaso FU, Coupe SJ, Charlesworth SM, Nnadi EO, 2013, Laboratory-Based Experiments to Investigate the Impact of Glyphosate-Containing Herbicide on Pollution Attenuation and Biodegradation in a Model Pervious Paving System, Chemosphere, 90, 737-746.

McCain GN, Suozzo MJ, Dewoolkar MM, 2010, A Laboratory Study on the Effects of Winter Surface Applications on the Hydraulic Conductivity of Porous Concrete Pavements” Transportation Research Board 2010 Annual Meeting CD-ROM.

Mohammed, B. S., Nuruddin, M. F., and Dayalan, Y. A. P. 2013, Apr. High permeable concrete incorporating pozzolanic materials-An experimental investigation. In Business Engineering and Industrial Applications Colloquium (BEIAC), 2013 IEEE (pp. 657-661). IEEE.

Montes F. and Haselbach L. 2006, Measuring Hydraulic Conductivity in Pervious Concrete, Environmental Engineering Science, 23(6), 960-969.

Morgenroth J and Buchan GD, 2009, Soil Moisture and Aeration beneath Pervious and Impervious Pavements, Arboriculture and Urban Forestry, 35(3), 135–141.

Morgenroth J, Buchan GD, and Scharenbroch BC, 2013, Belowground Effects of Porous Pavements-Soil Moisture and Chemical Properties, Ecological Engineering, 51, 221-228.

Neithalath N., Weiss J, and Olek J, 2006, Characterizing Enhanced Porosity Concrete Using Electrical Impedance to Predict Acoustic and Hydraulic Performance, Cement and Concrete Research, 36, 2074–2085.

Neithalath N., 2007, Extracting the Performance Predictors of Enhanced Porosity Concretes from Electrical Conductivity Spectra. Cement and Concrete Research. 37, 796-804.

Neithalath N., Weiss J, and Olek J, Predicting the Permeability of Pervious Concrete (Enhanced Porosity Concrete) from Non-Destructive Electrical Measurements, Presented online: https://fp.auburn.edu/heinmic/perviousconcrete/Porosity.pdf

Neithalath N, Bentz DP, and Sumanasooriya MS. 2010a, Predicting the Permeability of Pervious Concrete - Advances in characterization of pore structure and transport properties. Concrete international, May. 35-40.

Neithalath N, Sumanasooriya MS, Deo O, 2010b, Characterizing Pore Volume, Sizes, and Connectivity in Pervious Concretes for Permeability Prediction. Materials Characterization. 61, 802-813.

Offenberg M. 2005, Producing Pervious Pavements-Hints for the engineer, contractor on placement of pervious concrete. Concrete International, Mar. 2005, 50-54.

Putman BJ, Neptune AI, 2011, Comparison of test specimen preparation techniques for pervious concrete pavements. Construction and Building Materials, 25, 3480–3485.

Rehder, B., Banh, K., and Neithalath, N. 2014. Fracture behavior of pervious concretes: The effects of pore structure and fibers. Engineering Fracture Mechanics, 118, 1-16.

Rizvi R, Tighe S, Henderson V, and Norris J. 2010, Evaluating the Use of Recycled Concrete Aggregate in Pervious Concrete Pavement. Transportation Research Record: Journal of the Transportation Research Board, No. 2164, Transportation Research Board of the National Academies, Washington, D.C., 2010, pp. 132-140.

Sansalone J, Kuang X, Ying G, Ranieri V, 2012, Filtration and Clogging of Permeable Pavement Loaded by Urban Drainage, Water Research, 46, 6763-6774.

Schaefer, V.R., K. Wang, M.T. Suleiman, and J.T. Kavern, 2006, Mix Design Development for Pervious Concrete in Cold Weather Climates.Iowa DOT Final Report No. 2006-01.

Schaefer VR, Kevern JT, Lzevbekhai B, Wang K, Cutler HE, and Wiegand P. 2010, Construction and Performance of Pervious Concrete Overlay at Minnesota Road Research Project. Transportation Research Record: Journal of the Transportation Research Board, No. 2164, Transportation Research Board of the National Academies, Washington, D.C., pp. 82–88.

Schaefer VT and Kevern JT, 2011, An Integrated Study of Pervious Concrete Mixture Design for Wearing Course Applications, A final report prepared for Federal Highway Administration, U.S. Department of Transportation.

Scholz M, Grabowiecki P, 2007, Review of Permeable Pavement Systems. Building and Environment, 42, 3830-3836.

Schwartz SS, 2010, Effective Curve Number and Hydrologic Design of Pervious Concrete Storm-Water Systems. Journal of Hydrologic Engineering. Jun. 465-474.

Shen S, Burton M, Jobson B, Haselbach L. 2011, Pervious Concrete with Titanium Dioxide as a Photocatalyst Compound for a Greener Urban Road Environment, A final report prepared for the United States Department of Transportation.

Shen S, Burton M, Jobson B, Haselbach L. 2012, Pervious Concrete with Titanium Dioxide as a Photocatalyst Compound for a Greener Urban Road Environment, Construction and Building Materials 35, 874–883.

Shen, W., Shan, L., Zhang, T., Ma, H., Cai, Z., and Shi, H. 2013. Investigation on polymer–rubber aggregate modified porous concrete. Construction and Building Materials, 38, 667-674.

Shu X, Huang BS, Wu H, Dong Q, Burdette EG., 2011, Performance Comparison of Laboratory and Field Produced Pervious Concrete Mixtures. Construction and Building Materials, 25, 3187-3192.

Sonebi M, and Bassuoni M, 2013, Investigating the Effect of Mixture Design Parameters on Pervious Concrete by Statistical Modeling, Construction and Building Materials, 38, 147-154.

Sriravindrarajah R, Do HM, Nguyen LD, and Aoki Y. 2011, Effect of clogging on the water permeability of pervious concrete. Incorporating Sustainable Practice in Mechanics of Structures and Materials-Fragomeni, Venkatesan, Lam and Setunge (eds). 873-876.

Starke P, Göbel P, and Coldewey WG., 2010, Urban Evaporation Rates for Water-Permeable Pavement, Water Science and Technology-WST, 62(5), 1161-1169.

Starke P, Göbel P, and Coldewey WG., 2011, Effects on Evaporation Rates from Different Water-Permeable Pavement Designs. Water Science and Technology. 63.11, 2619-2627.

Suleiman, MT, Kevern, J, Schaefer, VR, and Wang K, Effect of Compaction Energy on Pervious Concrete Properties. Presented online: http://www.rmc-foundation.org/images/PCRC%20Files/Construction%20Techniques/Effect%20of%20Compaction%20Energy%20on%20Pervious%20Concrete%20Properties.pdf

Sumanasooriya MS, Bentz DP, and Neithalath N, 2009, Predicting the Permeability of Pervious Concretes from Planar Images. NRMCA Concrete Technology Forum: Focus on Performance Prediction. May 13-15, pp. 11.

Sumanasooriya MS and Neithalath N. 2011, Pore Structure Features of Pervious Concretes Proportioned for Desired Porosities and Their Performance Prediction, Cement and Concrete Composites, 33, 778-787.

Sumanasooriya MS, Deo O, and Neithalath N. 2012, Particle Packing-Based Material Design Methodology for Pervious Concretes. ACI Materials Journal, 109(2), March-April, 205-214.

Tawatchai T, Sata V, Chindaprasirt P, Jaturapitakkul C, 2012, Pervious High-Calcium Fly Ash Geopolymer Concrete. Construction and Building Materials, 30, 366-371.

Tennis PD, Leming ML, and Akers DJ. 2004, Pervious Concrete Pavement. Portland Cement Association. PCA Serial No. 2828.

Tian, B., Liu, Y., Niu, K., Li, S., Xie, J., and Li, X. 2013. Reduction of Tire-Pavement Noise by Porous Concrete Pavement. Journal of Materials in Civil Engineering, 26(2), 233-239.

Tyner JS, Wright WC, Dobbs PA., 2009, Increasing Exfiltration from Pervious Concrete and Temperature Monitoring. Journal of Environmental Management, 90, 2636-2641.

Ullate EG, Lopez EC, Fresno DC, Bayon JR. 2011, Analysis and Contrast of Different Pervious Pavements for Management of Storm-Water in a Parking Area in Northern Spain. Water Resour Manage, 25,1525–1535.

Vancura ME, MacDonald K, Khazanovich L. 2011a, Microscopic Analysis of Paste and Aggregate Distresses in Pervious Concrete in a Wet, Hard Freeze Climate. Cement and Concrete Composites, 33, 1080-1085.

Vancura ME, MacDonald K, Khazanovich L. 2011b, Structural Analysis of Pervious Concrete Pavement, Transportation Research Record: Journal of the Transportation Research Board, No. 2226, Transportation Research Board of the National Academies, Washington, D.C., pp. 13–20.

Vancura ME, MacDonald K, and Khazanovich L. 2012, Location and Depth of Pervious Concrete Clogging Material before and after Void Maintenance with Common Municipal Utility Vehicles. Journal of Transportation Engineering, 138, 332-338.

Volder A, Watson T, Viswanathan B , 2009, Potential Use of Pervious Concrete for Maintaining Existing Mature Trees During and after Urban Development, Urban Forestry and Urban Greening, 8, 249-256.

Wanielista M, Chopra M, Spence J, Ballock C. 2007, Hydraulic Performance Assessment of Pervious Concrete Pavements for Stormwater Management Credit. A final report prepared for the Florida Department of Transportation, Orlando, FL.

Wang K, Schaefer VR, Kevern JT., and Suleiman MT. Development of Mix Proportion for Functional and Durable Pervious Concrete. NRMCA Concrete Technology Forum: Focus on Pervious Concrete, May 24-25, 2006, Nashville, TN.

Wang ZJ, Du XQ, Yang YS, Ye XY, 2012, Surface Clogging Process Modeling of Suspended Solids during Urban Stormwater Aquifer Recharge, Journal of Environmental Sciences, 24(8), 1418-1424.

Welker AL, Barbis JD, and Jeffers PA. 2012, A Side-By-Side Comparison of Pervious Concrete and Porous Asphalt. Journal of the American Water Resources Association. 48(4), 809-819.

Wu H, Huang B, Shu X, Dong Q, Shrum E, Jared D, and Wu P, 2010, Laboratory Evaluation of Latex-Modified Pervious Concrete, Transportation Research Board, 2010 Annual Meeting.

Wu H, Huang BS, Shu X, and Dong Q. 2011, Laboratory Evaluation of Abrasion Resistance of Portland cement Pervious Concrete. Journal of Materials in Civil Engineering, May, 697-702.

Yakima County website, Regional Stormwater Management Program, Project: Low Impact Development Demonstration Project, http://www.yakimacounty.us/stormwater/LID/project.htm

Yang, Z, 2011, Freezing-and-Thawing Durability of Pervious Concrete under Simulated Field Conditions, ACI Materials Journal, 108(2), March-April, 187-195.

Yang Z, Brown H, and Cheney A, Influence of Moisture Conditions on Freeze and Thaw Durability of Portland cement Pervious Concrete. Presented online : http://www.rmc-foundation.org/images/PCRC%20Files/Durability%20&%20Maintenance/Influence%20of%20Moisture%20Conditions%20on%20Freeze%20and%20Thaw%20Durabiltity%20of%20Portland%20Cement%20Pervious%20Concrete.pdf

Yong CF, McCarthy DT, Deletic A, 2013, Predicting Physical Clogging of Porous and Permeable Pavements, Journal of Hydrology, DOI: http://dx.doi.org/10.1016/j.jhydrol.2012.12.009

Zaldo, M. 2006, Pervious Concrete Pavements Industry Focus, National Ready Mixed Concrete Association, presented on line: www.NRMCA.org

Chapter 4 Field Performance of Pervious Concrete Sections

The field testing consisted of 1) an infiltration rate test by using ASTM C1701 "*Standard Test Method for Infiltration Rate of in Place Pervious Concrete*" at five or more locations within each case study, and 2) a pavement condition survey performed by an FHWA-certified technician. A lab simulation study by Haselbach (2006) revealed that "*extreme events with substantial deposition of clay (in runoff) on a pervious concrete pavement will substantially reduce its service capability, even temporarily fully clogging the pavement*." However, sweeping and rinsing (e.g., subsequent rainfall) restored permeability to acceptable levels. As such, infiltration will be measured after winter maintenance operations and before and after sweeping or vacuum maintenance.

Two sections of pervious concrete were installed as part of the construction of the Mt Rose Highway Water Quality Improvement Project (NDOT Project #MS-0431 [006] Contract #3501 on SR 431) and the Hwy 28 Improvement Project (NDOT Project # SI-0028 [007] Contract #3471 on SR28), both in Incline Village, Nevada (Lake Tahoe). In addition, prior to the project construction, a test panel was installed in Reno, Nevada. The Mt Rose section (Area A) is approximately 20 ft wide by 625 ft long and was installed along the southern edge of Mt Rose highway northeast of College Drive. Secondly, an approximately 20 ft wide by 350 ft long section was installed along the northern edge of State Route 28 west of Ponderosa Ave (Area B). NCE observed construction of the pervious concrete test panel and construction of the two pervious concrete infiltration structures in the summer of 2012. After the concrete had cured, NCE performed baseline distress surveys and infiltration testing of the pervious concrete.

The slump, density, air void content, compressive and tensile strengths of the freshly mixed pervious concrete were tested according to ASTM C143, C1688, C39, and C496, respectively. The results are shown in Table 4.1. As displayed in the table, the slump of the freshly mixed pervious concrete was 1/4 inch, the unit weight was 123.2 PCF, the total air voids was 22.8%, the average 7d and 28d compressive strengths were 2770 and 3330 psi, respectively, and the average 7d and 28d tensile strengths were 300 and 315 psi, respectively.

The drainage of soil and roadway configuration (e.g., steep slope) were examined and documented in the field testing of pervious concrete pavement. The infiltration was calculated according to the following equation:

$$\mathrm{I} = \frac{KM}{(D^2)(t)} \tag{4.1}$$

where I is the infiltration rate (in/hr), M is the mass of the infiltrated water (lb), D is the infiltration ring inside diameter (in), t is the time required for water to infiltrate concrete (sec), and K is a constant (126.870 in-pounds)

Table 4.2 gives the infiltration field testing results in two areas. The freshly mixed pervious concrete has an average infiltration rate of 0.3-0.4 in/sec; however, after one year of service, the infiltration rate was reduced to 0.1-0.01 in/sec.

Table 4. 1 The properties of the freshly mixed pervious concrete

(Report from *Construction Materials Engineers, INC*.)

TEST RESULTS	
Slump (ASTM C143)	¼ Inch
Unit Weight (ASTM C1688)	123.2 PCF
Target Unit Weight (ASTM C1688)	118.2 PCF – 128.2 PCF
Total Voids (ASTM C1688)	22.8%
Average Compressive Strength (ASTM C39)*	
7 Day	2770 PSI
28 Day	3330 PSI
Average Tensile Strength (ASTM C496)*	
7 Day	300 PSI
28 Day	315 PSI

*Note: The test cylinders were molded with the same compaction hammer and similar effort as outlined in ASTM C1688.

Table 4. 2 Infiltration field testing results

NDOT - Mt Rose Hwy WQIP											
Incline Village, NV											
Area	**Station**	**Offset from CL**	**Material**	**Date**	**Infiltration Rate (in/s)**	**Date**	**Infiltration Rate (in/s)**	**Date**	**Infiltration Rate (in/s)**	**Date**	**Infiltration Rate (in/s)**
A	0+75	25	PCC	2012/10/18	0.432	2013/ 5/21	0.095	NA		2013/11/ 11	0.036
A	3+13	39	sand	2012/9/17	0.027	NA	NA	NA		NA	NA
A	3+13	39	3/4" drain rock	2012/9/17	0.656	NA	NA	NA		NA	NA
A	3+13	39	PCC	2012/10/18	0.366	2013/ 5/21	0.064	2013/ 5/21	0.204	2013/11/ 11	0.144
A	3+13	31	PCC	2012/10/18	0.400	2013/ 5/21	0.017	NA	NA	2013/11/ 11	0.099
A	3+13	22	PCC	2012/10/18	0.307	2013/ 5/21	0.014	2013/ 5/21	0.150	2013/11/ 11	0.039
A	5+50	23.5	PCC	2012/10/18	0.330	2013/ 5/21	0.007	NA	NA	2013/11/ 11	0.018
B	0+50	18	PCC	2012/10/18	0.391	2013/ 5/21	0.082	NA	NA	2013/11/ 11	0.009
B	0+50	29	PCC	2012/10/18	0.424	2013/ 5/21	0.229	NA	NA	2013/11/ 11	0.265
B	1+20	29.5	sand	2012/9/20	0.041	NA	NA	NA	NA	NA	NA
B	1+20	29.5	3/4" drain rock	2012/9/20	1.015	NA	NA	NA	NA	NA	NA
B	1+76	17	PCC	2012/10/18	0.450	2013/ 5/21	0.016	2013/ 5/21	0.237	2013/11/ 11	0.017
B	1+76	28	PCC	2012/10/18	0.411	2013/ 5/21	0.220	2013/ 5/21	0.208	2013/11/ 11	0.190
B	3+00	17	PCC	2012/10/18	0.377	2013/ 5/21	0.002	NA	NA	2013/11/ 11	0.007
B	3+00	28	PCC	2012/10/18	0.353	2013/ 5/21	0.009	NA	NA	2013/11/ 11	0.004
(cyan)	pervious PCC test result										
(orange)	location was swept with vacuum sweeper and immediately re-tested										

4.1 Maintenance Activities

Maintenance Activities

The details of the maintenance activities will be provided by NCE. At the time of NCE's initial infiltration testing in mid-October, 2012, no maintenance activities such as brooming, sweeping, or vacuum sweeping had been performed on the concrete sections. Because the winter snow season had not yet started, no traction sand had yet been applied to the highways.

During the winter months, the traction sand was applied to the asphalt highway surfaces at both locations. The quantity and timing of traction sand application was dependent upon the duration and severity of winter storm events. Traction sand application rates and timing cannot be predicted at this time. The de-icing compounds such as salt was applied to the asphalt highway surfaces at both locations. Maintenance activities such as street sweeping and vacuuming were performed by NDOT maintenance crews within the project area. Snow plows and snow removal equipment with tire chains were subjected the slabs to greater load weights as well as cracking.

Key findings:

- The slump of the freshly mixed pervious concrete was 1/4 inch, the unit weight was 123.2 PCF, the total air voids was 22.8%, the average 7d and 28d compressive strengths were 2770 and 3330 psi, respectively, and the average 7d and 28d tensile strengths were 300 and 315 psi, respectively.
- The freshly mixed pervious concrete has an average infiltration rate of 0.3-0.4 in/sec; however, after one year of service, the infiltration rate was reduced to 0.1-0.01 in/sec.

Chapter 5 Laboratory Investigation

5.1 Introduction

Cores from the field sites were collected by NDOT and NCE and shipped to WTI for laboratory testing. Locations for the coring were situated throughout the length of the test sites at various distances from the pavement edge. The cores were also collected from areas identified as having various levels of distress (*limited*, *moderate* or *severe*). A total of 18 cores from the SR28 site and 22 cores from the SR431 site were collected, as shown in Table 5.1. Cores from SR431 were collected on May 20, 2013, cores from SR28 were collected on May 21, 2013, and slabs were harvested on May 23, 2013 for both sites. Tests to evaluate engineering properties of the constructed test sections used the limited distress cores, in addition to two slabs from each site. A secondary investigation looking at the concrete microstructure used the distressed cores as well.

The typical engineering properties of interest for traditional concrete and pervious concrete were tested in general accordance to ASTM standards. Since pervious concrete features interconnected voids between aggregates (and thus high porosity and permeability), its strength and durability are of significant concern. Compressive and tensile strength are important with respect to cracking, shear capacity, anchorage capacity, and durability. The tensile strength of the concrete samples was determined by testing the splitting tensile strength of cylinders (ASTM 496). The compressive strength of concrete cylinders was determined according to ASTM C39 (*Test Method for Compressive Strength of Cylindrical Concrete Specimens*).

Durability of the pervious concrete samples was assessed by abrasion resistance, and freeze–thaw and salt-scaling resistance tests. The abrasion resistance of the cores was determined following ASTM C1747 (*Test Method for Determining Potential Resistance to Degradation of Pervious Concrete by Impact and Abrasion*), which uses the Los Angeles abrasion machine without the steel charge used for aggregate durability. The freeze-thaw and salt scaling of concrete slabs was evaluated following the BNQ NQ 2621-9010 (2002 standard of the Province of Quebec, Canada), as this is a laboratory test method better representative of the field conditions than the ASTM C672.

Absorption capacity is an indicator of a concrete's resistance to degradation from various environmental exposures, as much of this degradation is associated with the ingress of moisture into the hardened concrete. As such, absorption properties of the concrete cores were determined using the test methods outlined in ASTM C642 (*Test Method for Density*, *Absorption, and Voids in Hardened Concrete*), which involves submerging dry test specimens and monitoring their weight change over time. Alternatively, the total porosity of cored pervious concrete samples was measured following the water displacement method developed by Montes (2005).

Performance tests consisted of drainage testing to assess infiltration rate. A falling head permeability test was designed based on examples identified during the literature review (McCain, 2010;

Huang, 2010; Rizvi, 2010, and Schaefer, 2006). The field cores were trimmed and initially tested with clean water to provide baseline infiltration rates, reported in drain-down time and hydraulic conductivity. Then, tests were conducted using simulated storm water runoff with fine particulates and applications of traction sand. Any reduction in infiltration rate was recorded, as well as any reduction in the total solids content of the effluent water.

An investigation of the microstructure of the cores of various distress levels was conducted to help explain the differences between SR28 and SR431. This investigation used a scanning electron microscope and micro computed X-ray tomography device.

Table 5. 1 Location of cores within each test site

SR 28				**SR431**			
Core No.	Station Location[-1-]	Offset from Pavement Edge	Level of Distress	Core No.	Station Location	Offset from Pavement Edge	Level of Distress
SR28-1	0+21.5	11'	Limited	SR431-1	0+62	3'	Severe
SR28-2	0+39.5	4'	Limited	SR431-2	0+81	6'	Limited
SR28-3	0+57	7.5'	Limited	SR431-3	1+08.5	5.5'	Moderate
SR28-4	0+75	13.5	Limited	SR431-4	1+26	5.5'	Severe
SR28-5	0+94.5	9.5'	Limited	SR431-5	1+66	3'	Severe
SR28-6	1+14.5	2.5'	Moderate	SR431-6	1+84	11.5'	Limited
SR28-7	1+33.5	5.5'	Limited	SR431-7	2+14.5	9.5'	Limited
SR28-8	1+52.5	15'	Limited	SR431-8	2+46	7.5'	Limited
SR28-9	1+71.5	6.5'	Limited	SR431-9	2+62.5	15.5'	Limited
SR28-10	1+84.5	4.5'	Severe	SR431-10	2+75	11'	Limited
SR28-11	2+11.5	2'	Severe	SR431-11	2+90	4'	Limited
SR28-12	2+30.5	9.5'	Limited	SR431-12	3+15	14'	Limited
SR28-13	2+47.5	13'	Limited	SR431-13	3+42	9'	Limited
SR28-14	2+66.5	4.5	Moderate	SR431-14	3+49	1'	Severe
SR28-15	2+85	1.5'	Limited	SR431-15	3+69	12.5'	Limited
SR28-16	3+00	10'	Limited	SR431-16	3+93	9'	Limited
SR28-17	3+18.5	5'	Limited	SR431-17	4+20	11'	Moderate
SR28-18	3+42.5	4.5	Limited	SR431-18	4+46	3.5'	Moderate
				SR431-19	4+67	5.5'	Moderate
				SR431-20	4+85	8'	Moderate
				SR431-21	5+10	2	Limited
				SR431-22	5+45	3'	Severe
Slab #				**Slab #**			
SR28-1	1+04	14.5'	Limited	SR431-1	2+36.5	15'	Limited
SR28-2	2+53.5	7.5'	Limited	SR431-2	3+52	16'	Limited

[-1-]Stations start from the East end (0+00) heading west

5.2 Engineering Properties

5.2.1 Overview of results

A summary of the results of the strength, durability, and performance testing is provided in Table 5.2. In general the strength and durability of SR28 was better than SR431, which is consistent with field observations. The hydraulic conductivity of SR431 was greater than SR28, but both were sufficient to promote drainage.

Table 5. 2 Summary of Durability, Strength and Hydraulic Performance

Standard	Property	SR28		SR431	
		Average	**Std Dev**	**Average**	**Std Dev**
ASTM C39	Compressive Strength (psi)	908	95	762	62
ASTM C496	Splitting Tensile Strength (psi)	276	19.2	183	47
ASTM C1747	Abrasion Resistance (% mass loss)	48.3		59.2	
ASTM C642	Density (lb/ft^3)	104.2	4.6	102	12.6
	Air Voids/Porosity (%)	34.5	3.1	36.2	7.9
	Water Absorption (%)	3.3	0.25	4	0.13
N/A	Hydraulic Conductivity (in/sec)	0.44	0.06	0.53	0.03
BNQ NQ 2621-9010	Salt Scaling Resistance (% mass loss)	27.24*	81.1*	90.35*	89.8*

*These values are results from individual samples, not an average and standard deviation.

5.2.2 Compressive strength

The results of the compressive strength tests are shown in Fig. 5.1. The samples cored from site SR28 exhibited a higher compressive strength than the samples from site SR431 (908 ± 95 psi and 762 ± 62 psi, respectively).

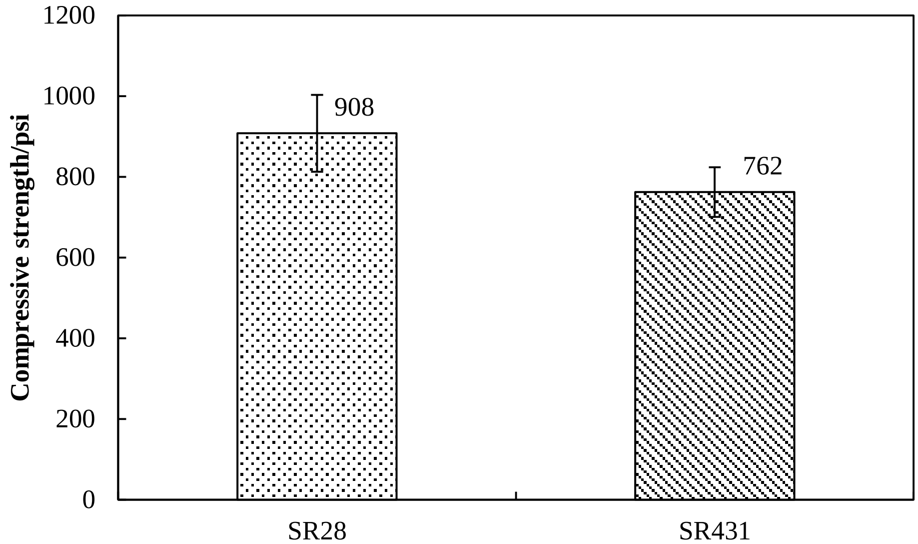

Fig. 5. 1 Average compressive strength (ASTM C39) of the samples cored from SR28 and SR431 with error bars showing ± one standard deviation

5.2.3 Splitting tensile strength

Splitting tensile strength (ASTM C496) results are shown in Fig. 5.2. Similar to the compressive strength testing results, higher strength was seen in the samples from SR28 than SR431 (276 ± 19.2 psi and 183 ± 47 psi, respectively).

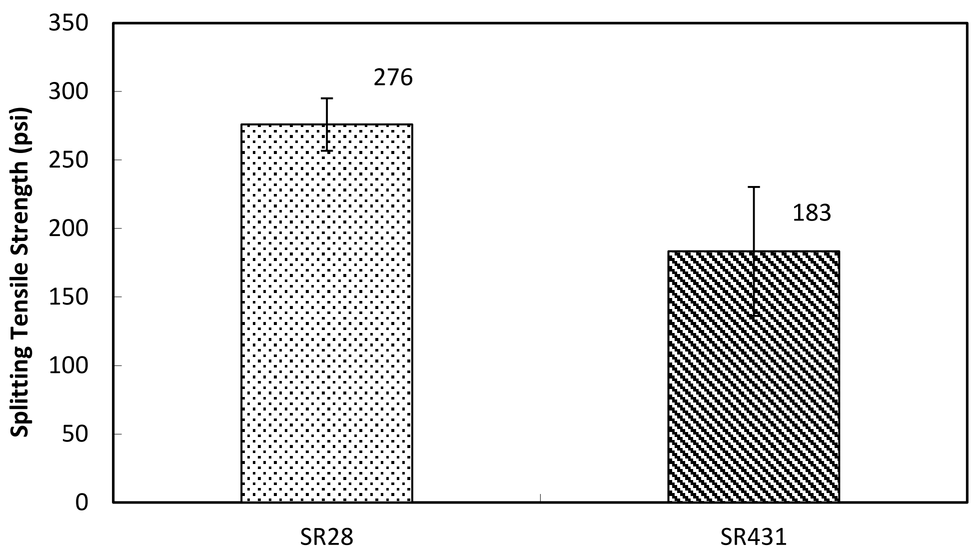

Fig. 5. 2 Splitting tensile strength of the samples cored from SR28 and SR431

5.2.4 Abrasion resistance

As might be expected based on the strength testing results, the stronger SR28 samples had less mass loss during the impact and abrasion resistance test than the SR431 samples (only 48% vs. 59%). This translates into an abrasion resistance for site SR28 that is more than 20% greater than site SR431.

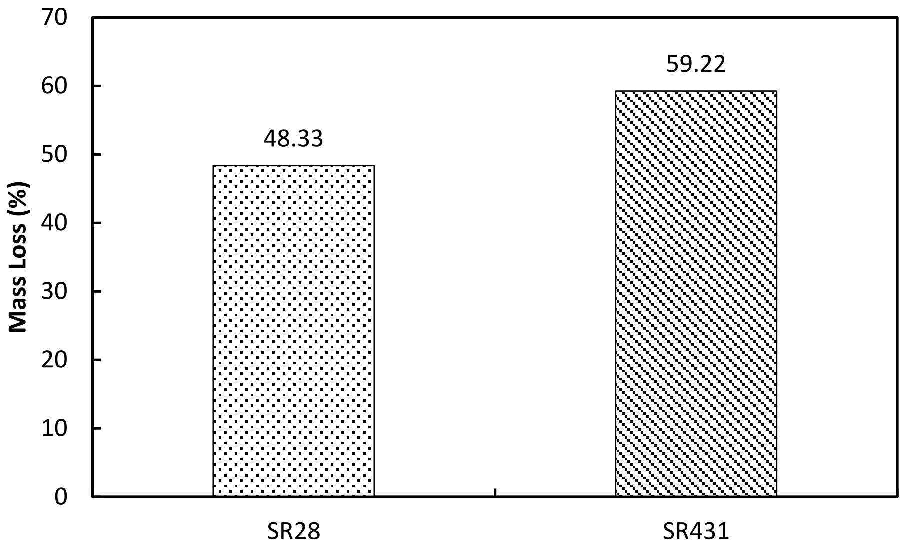

Fig. 5. 3 Abrasion resistance of the samples cored from SR28 and SR431

Note: Three samples from each site were tested. As per the testing standard, all three samples from a given site were tested simultaneously to determine a cumulative mass loss. The samples tested from site SR28 were 9, 13 and 17. The samples tested from site SR431 were 7 and two separate pieces of sample 8.

5.2.5 Density and air voids

The density testing results are shown in Fig. 5.4. As shown in this figure, the density difference between the two sites is not very obvious. The density of the samples from site SR28 has an average value of 104 ± 4.6 lbs/ft^3, while those from site SR431 have an average value of 102 ± 12.6 lbs/ft^3.

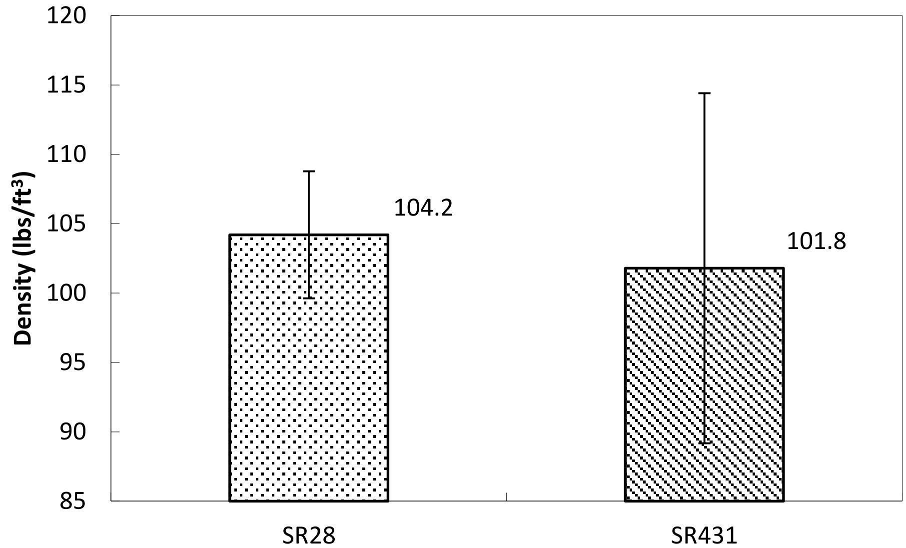

Fig. 5. 4 Density of the samples cored from SR28 and SR431

Similarly, the air void values of the samples cored from site SR28 and SR431 are very close, as shown in Fig. 5.4. The air voids of the samples from site SR28 had an average value of 34.5±3.1 %, while those from site SR431 had an average value of 36.2±7.9%.

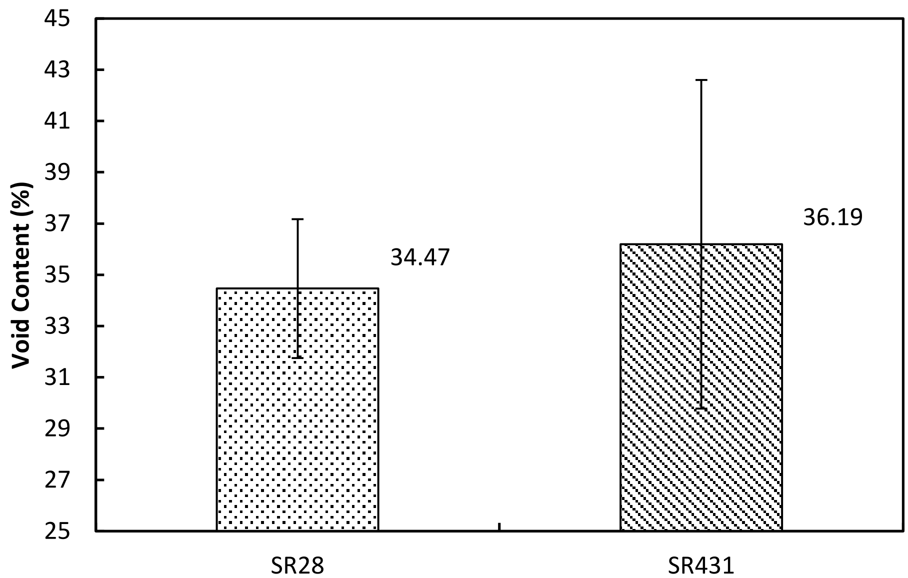

Fig. 5. 5 Void content of the samples cored from SR28 and SR431

Large deviations from the average in void content and density for samples from site SR431 indicate an issue with placement and compaction of the pervious concrete installation at that site. Both sites demonstrate a porosity much higher than required by the mix design. This is consistent with a lower than expected compressive strength for both sites. The higher porosity and lower density of site SR431 relative to site SR28 is also consistent with a lower compressive strength for site SR431 relative to site SR28.

5.2.6 Water Permeability

Although the values of the density and air voids are not remarkably different from these two sites, the SR28 samples still shows a higher density and lower air void content. As a result, it is not surprising that the hydraulic conductivity for samples from site SR431 is higher than for samples from site SR28, with values of 0.44 ± 0.06 in/sec and 0.53 ± 0.03 in/sec, respectively. This is consistent with the proportional relationship between the porosity and the permeability.

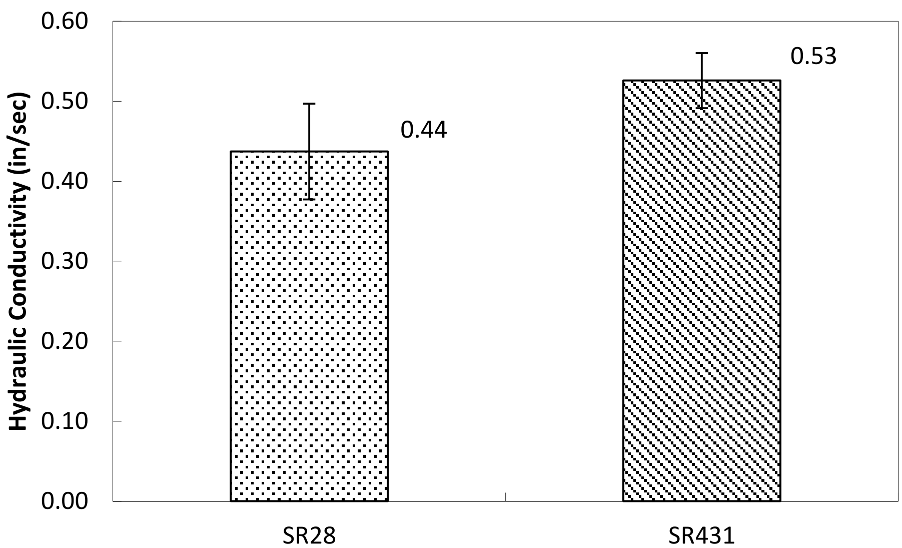

Fig. 5. 6 Hydraulic conductivity of the samples cored from SR28 and SR431

5.2.7 Water absorption

However, the water absorption difference of the samples cored from site SR28 and SR431 is relatively higher than the density and the air voids, as shown in Fig. 5.7. The water absorption of the samples from site SR28 has an average value of 3.3% ± 0.25%, while those from site SR431 have an average value of 4.0% ± 0.13%, which is over 20% higher than the SR28 samples.

Unlike the density and the air voids, which are largely governed by the macro pores (with size of centimeters to millimeters) of the samples, the value of the water absorption is largely determined by the micro pores (with size of micrometers to nanometers) of the samples. By combining the absorption testing results with the compressive strength and splitting tensile strength testing results, which have 20% and 50% variation rate between the SR28 and SR431, respectively, it can be concluded that the loss of the mechanical properties mostly resulted from the microstructure changes of the samples even without obvious macrostructure changes. This can be further demonstrated by the variation rates of the density and air voids, which have only 5% variations, while the water absorption and water permeability rates have variations greater than 20%.

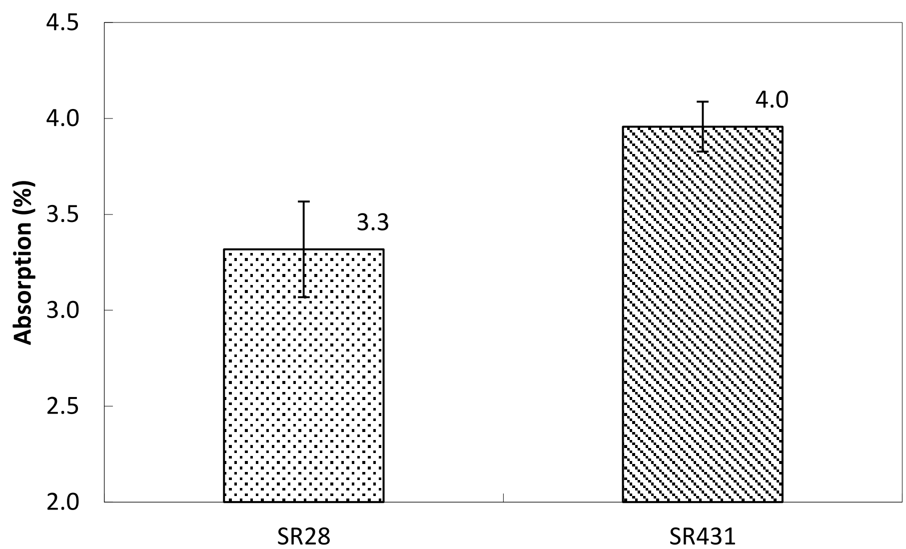

Fig. 5. 7 Water absorption of the samples cored from SR28 and SR431

5.2.8 Salt scaling

Fig. 5.8 shows the external dimensions of the samples experienced seven freeze/thaw cycles in 3% sodium chloride solution. As demonstrated in this figure, the external dimension of the SR28 sample is relatively well maintained, while the SR431 sample has more evident salt scaling than the SR28 samples. Fig. 5.9 demonstrates the mass loss of the samples extracted from site SR28 and site SR431 as a function of freeze/thaw cycles in a 3% sodium chloride solution. As illustrated in this figure, the mass loss of the samples from site SR28 is more stable than the samples from site SR431. After seven freeze/thaw cycles in the 3% sodium chloride solution, the mass losses of SR28 samples are 27.24% and 81.07%, as compared with 90.35% and 89.77% for the SR431 samples.

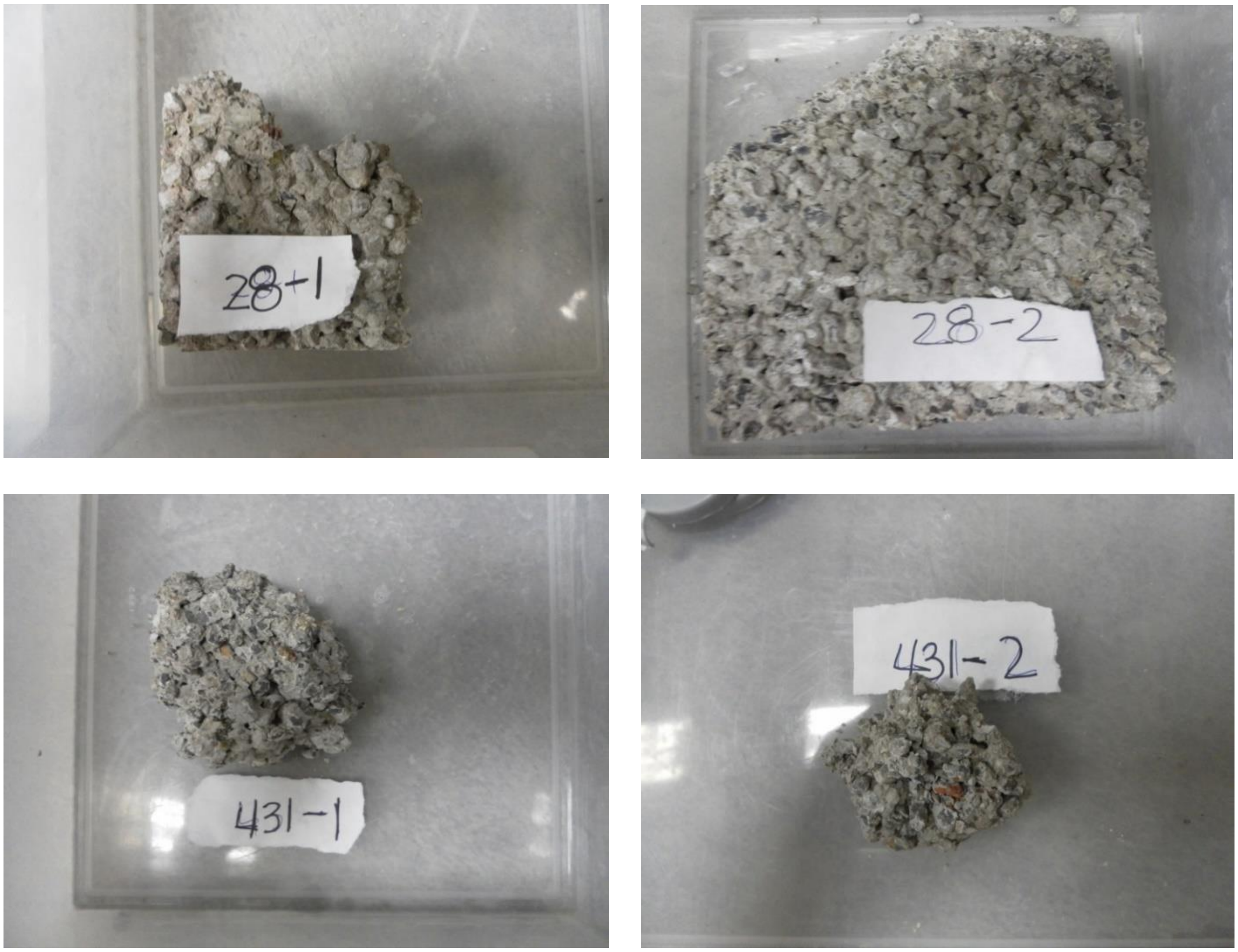

Fig. 5. 8 External dimension of the samples from SR28 and SR431, after experiencing 7 freeze/thaw cycles in 3% sodium solution.

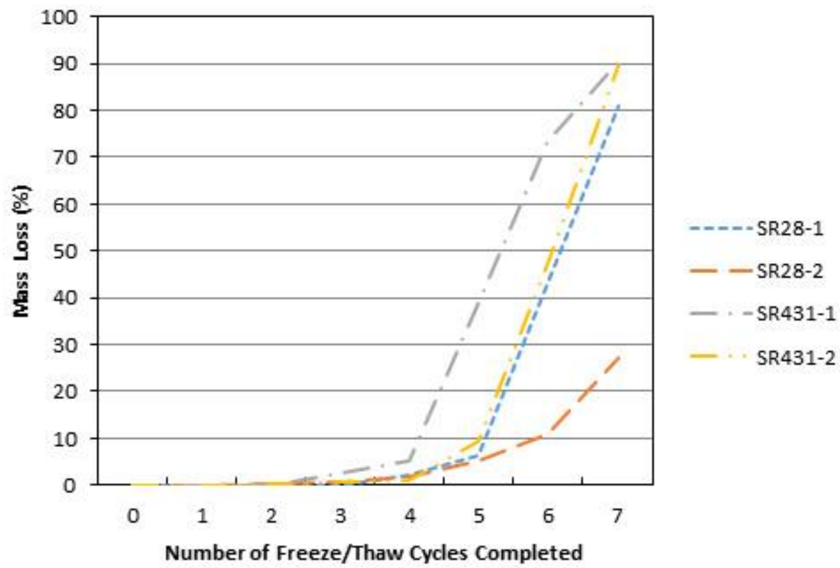

Fig. 5. 9 Mass loss of the samples harvested from site SR28 and site SR431 as a function of freeze/thaw cycles in a 3% sodium chloride solution

5.3 Microstructure investigation

As demonstrated above, the overall performance of the pervious concrete is largely determined by the microstructures. Therefore, the microstructure has to be analyzed to elucidate the real mechanisms of the performance degradation. In this section, scanning electron microscopy (SEM) and X-ray tomography (μCT) were used to analyze the microstructures and the 3D tomography of the samples cored from SR28 and SR431. The SEM was mainly applied to demonstrate the morphology of the cement paste at the interfaces between two aggregates, and the μCT was applied to show the porosity with a resolution of 10 μm and the 3D images of the samples.

5.3.1 SEM

The samples from both sites were divided into three categories, *limited*, *moderate*, and *severe*. Therefore, the samples were numbered as SR28-lim, SR28-mod, SR28-sev, SR431-lim, SR431-mod, and SR431-sev, respectively. The six types of samples from SR28 and SR431 were all observed by SEM.

Fig. 5.10 shows the low magnification fracture surface SEM morphologies of the samples cored from the SR431 site. In this figure, part a), b) and c) represent the *limited*, *moderate,* and *severe* conditions, respectively. In part a), the *limited* sample shows relatively good amorphous binder phase, although a few areas have become porous. In part b), however, some needle shape precipitates can be observed, and the quantity of the amorphous binder phase has been considerably reduced. Furthermore, as visible in part c), most of the amorphous cement paste binder phase has become porous structure, and a large number of small sized crystals were observed in the pores.

To illustrate more details of the microstructures, the high magnification fracture surface SEM morphologies of the samples cored from SR431 site are shown in Fig. 5.11. Again, part a), b) and c) represent the *limited*, *moderate*, and *severe* conditions, respectively. In part a), a small number of crystal sized particles were embedded in the binder phase, and some of the homogenous amorphous binder phase has become stripped in randomly orientated directions. In part b), a considerable number of needle shaped precipitates can be observed, although the content mainly consists of the homogenous amorphous binder phase. In part c), most of the amorphous cement paste binder phase has disappeared, and the needle shaped precipitates have grown to large sized crystals, and has become the main phase.

Fig. 5.12 demonstrates the high magnification SEM morphologies of the needle shaped precipitates, shown as part a), and the rod shaped crystals, shown as part b), from the *moderate* and *severe* conditions of samples from the SR28 site, respectively. In part a), the diameters of the needle shaped precipitates are about 100 nm, and the surfaces of some needles are smooth while others are not. A small amount of the binder phases, which mainly contributes the strength of the samples, are can still be observed in the needle agglomerates. However, as shown in part b), little binder phase can be observed, and large amount of crystals were observed instead of needle shaped precipitates. The size of the crystals were about 1 μm in diameter and 10 μm in length, and the axial direction of these small sized crystals are all perpendicular to the fracture surfaces. This is the reason why these samples show the lowest mechanical properties.

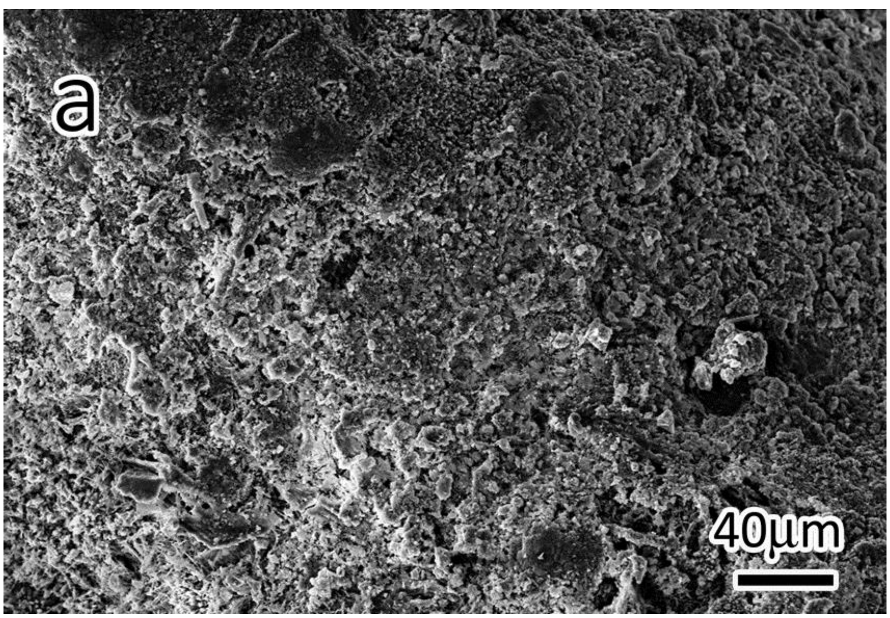

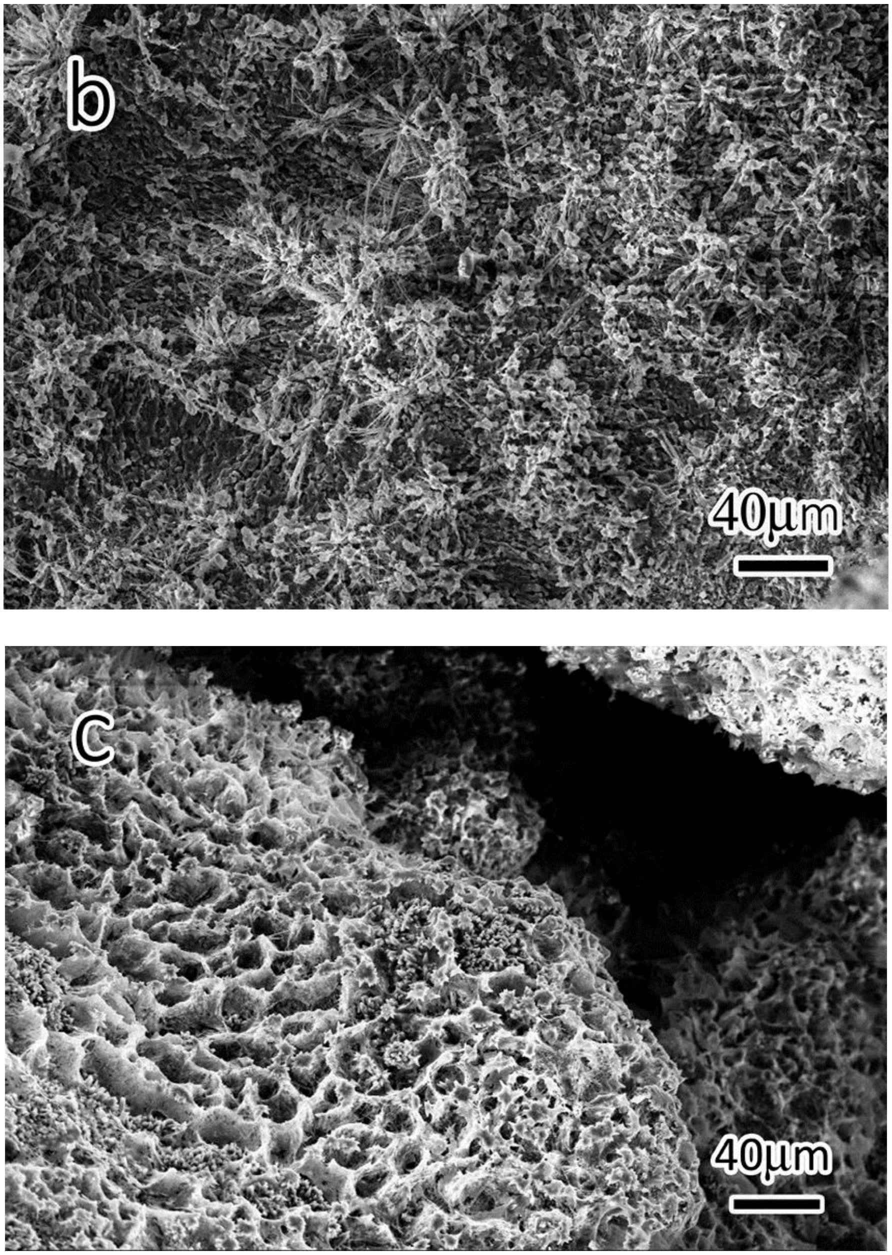

Fig. 5. 10 Low magnification fracture surface SEM morphologies of the samples cored from SR431 site a) limited, b) moderate, and c) severe.

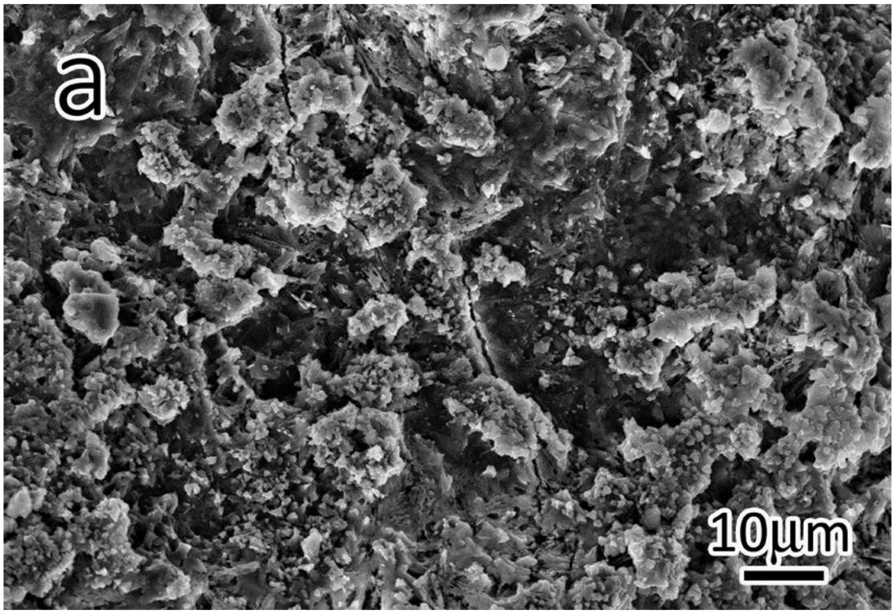
a
10μm

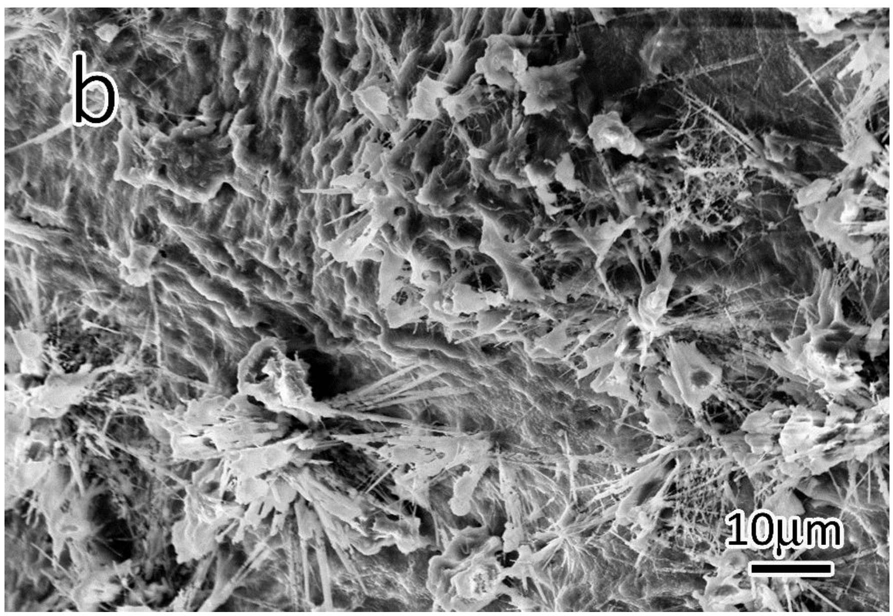
b
10μm

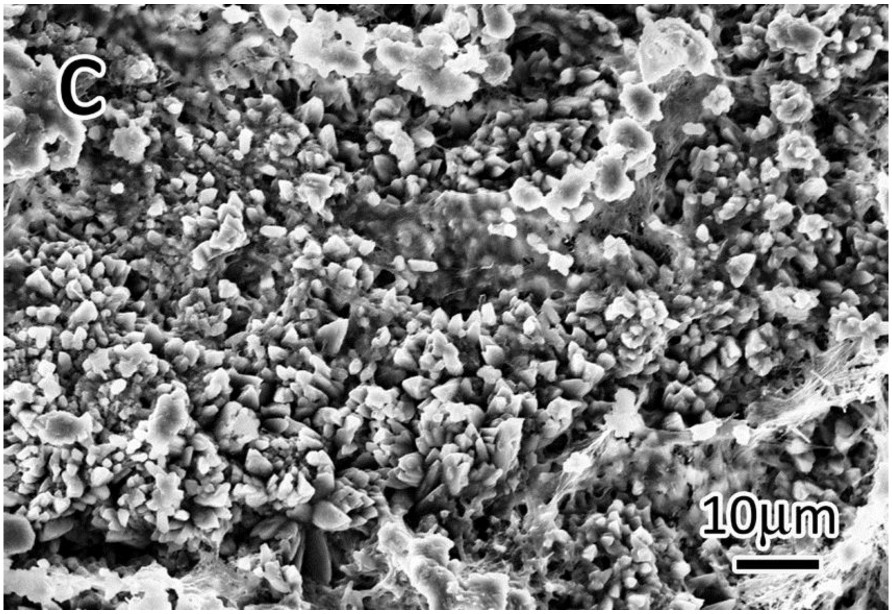

Fig. 5. 11 High magnification fracture surface SEM morphologies of the samples cored from SR431 site a) limited, b) moderate, and c) severe.

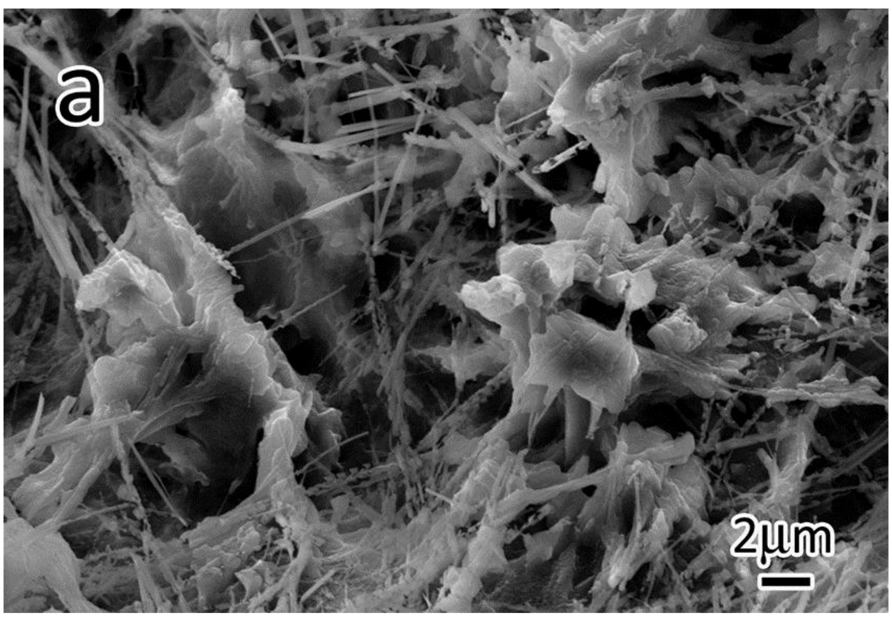

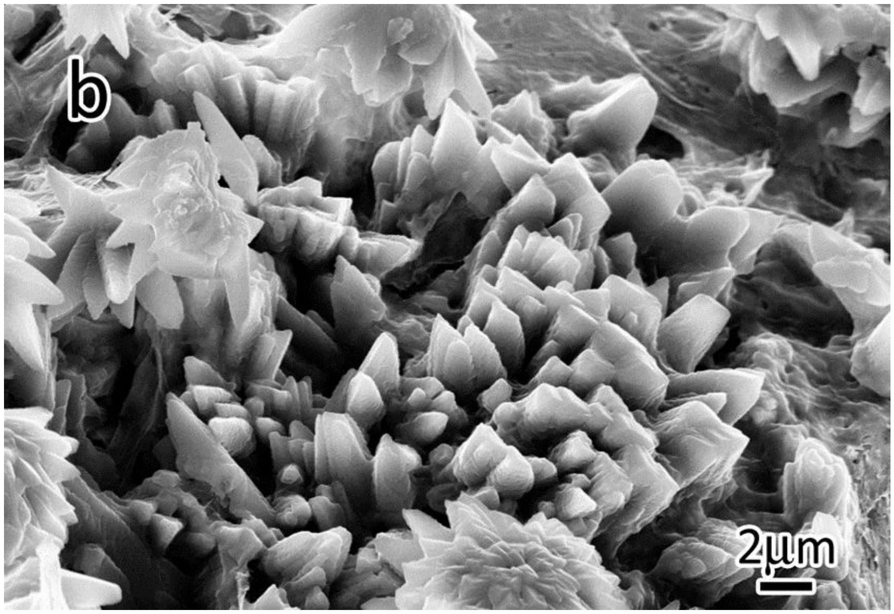

Fig. 5. 12 High magnification fracture surface SEM morphologies of the samples cored from SR431 site, a) moderate, and b) severe.

Similar to the samples from site SR431, the samples cored from site SR28 were also observed by SEM to demonstrate their microstructures. Fig. 5.13 shows the low magnification fracture surface SEM morphologies of the samples cored from the SR28 site. In this figure, part a), b) and c) represent the *limited, moderate*, and *severe* conditions, respectively. In the *limited* sample, shown as part a), the fracture surface shows a typical amorphous cement binder phase structure. The microstructures are almost in a dense condition without observable pores. The fracture surface is relatively smooth and no precipitates can be observed. In *moderate* samples; however, the surface is not as smooth as the limited one. Some homogeneously distributed precipitates can be observed, although the main binder phase is still the predominant phase. Similar to the samples from site SR431, the *severe* samples show very rough surfaces with a large number of crystals precipitates, shown as part c).

The high magnification fracture surface SEM morphologies of the samples cored from SR28 site are shown in Fig. 5.14. Again, part a), b) and c) represent the *limited, moderate,* and *severe* conditions, respectively. In part a), the amorphous cement phase are in a very good condition, and few precipitates can be observed in the binder phase. In part b), a small number of crystal sized particles embedded in the binder phase can be observed, and the quantity of the homogenous amorphous binder phase has reduced. In part c), most of the amorphous cement paste binder phase has disappeared, and the precipitated isometric crystals are the main phase of the samples, which is different from the samples cored from SR431. The average size of the isotropic crystals is about 1 μm. One thing to be noted here is that the microstructure of the samples from SR431-lim is very similar to the samples from SR28-mod, which has some nano sized precipitates embedded in the cement binder phase.

Fig. 5.15 demonstrates the enlarged high magnification SEM morphologies of the SR28-mod samples, shown as part a), and the isotropic precipitated crystals, shown as part b), from the *moderate* and *severe* conditions of samples from the SR28 site, respectively. In part a), a small number of isotropic crystals are embedded in the amorphous binder phase. However, as shown in part b), a large number of isotropic crystals were observed as the main phase, and little amorphous cement binder phase can be detected. The average size of the crystals was about 1 μm.

It is well established that the C-S-H cement phase is the main binder material that accounts for the strength of the concrete. In these pervious concrete samples, the differences in the overall performance are determined by their content of the C-S-H binder phase. As shown in the above figures, when the samples were changed from limited to severe, their microstructure has been changed from dense C-S-H phase to porous structure that was composed of small sized crystals, which largely reduce the bonding strength of the cement and resulted in the increasing of the air voids content, water absorption and permeability, and consequently, the splitting tensile strength, compressive strength, and the abrasion resistance were all decreased.

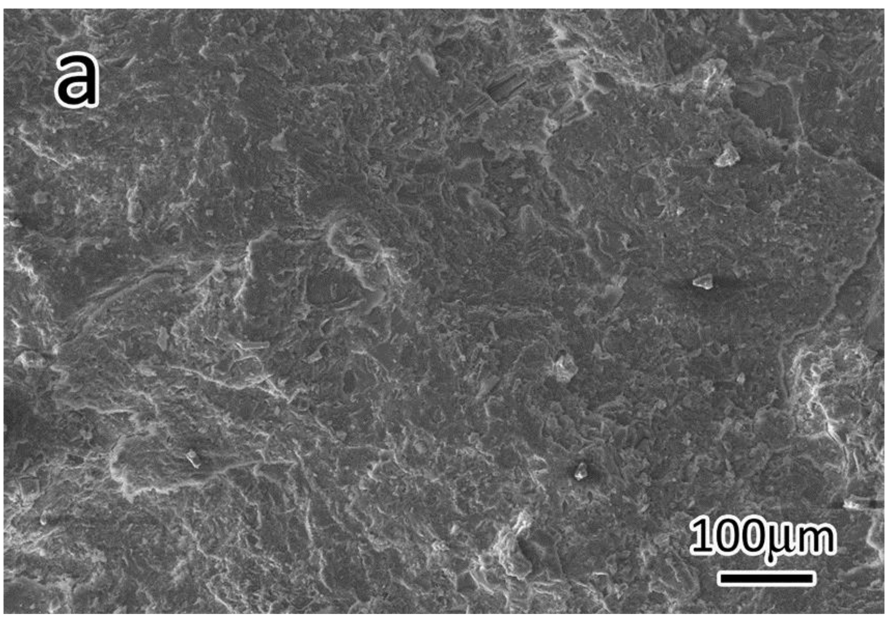

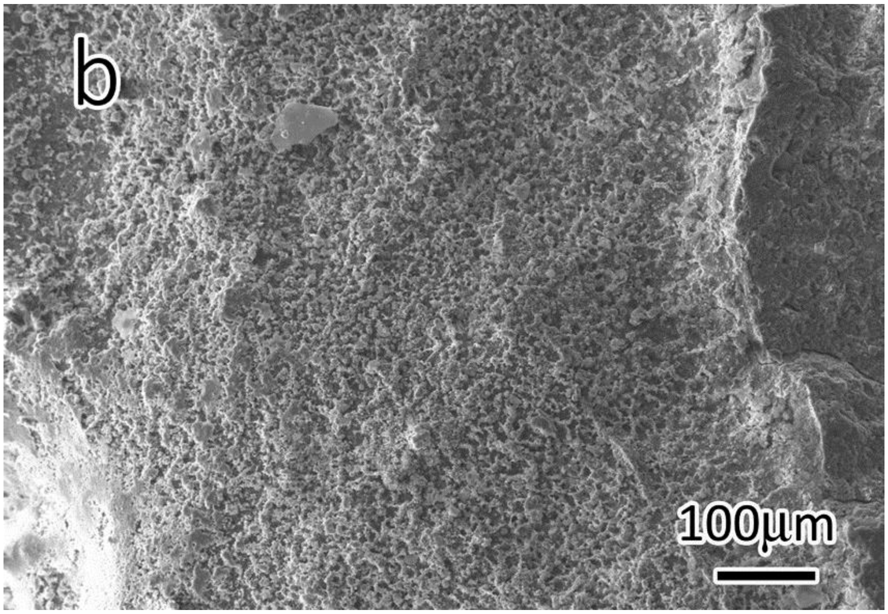

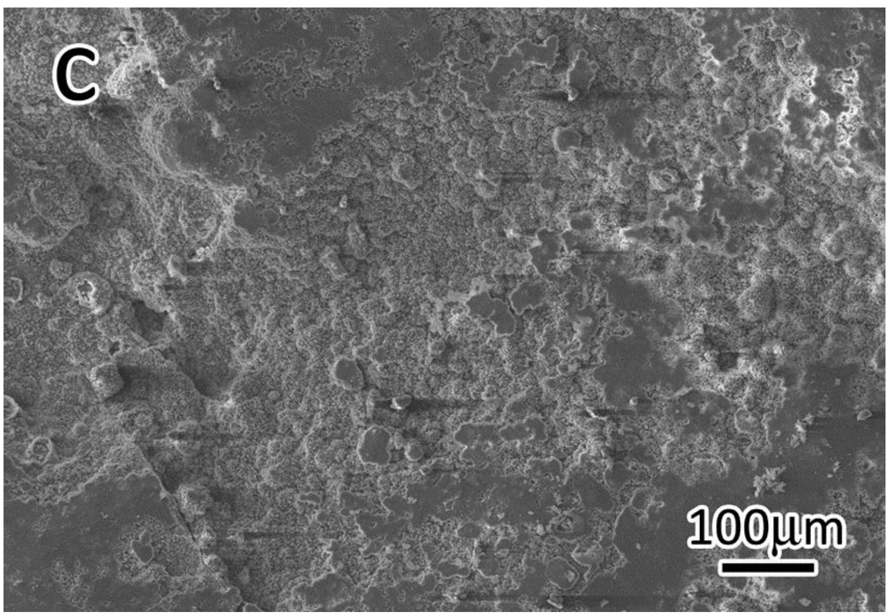

Fig. 5. 13 Low magnification fracture surface SEM morphologies of the samples cored from SR28 site, a) limited, b) moderate, and c) severe

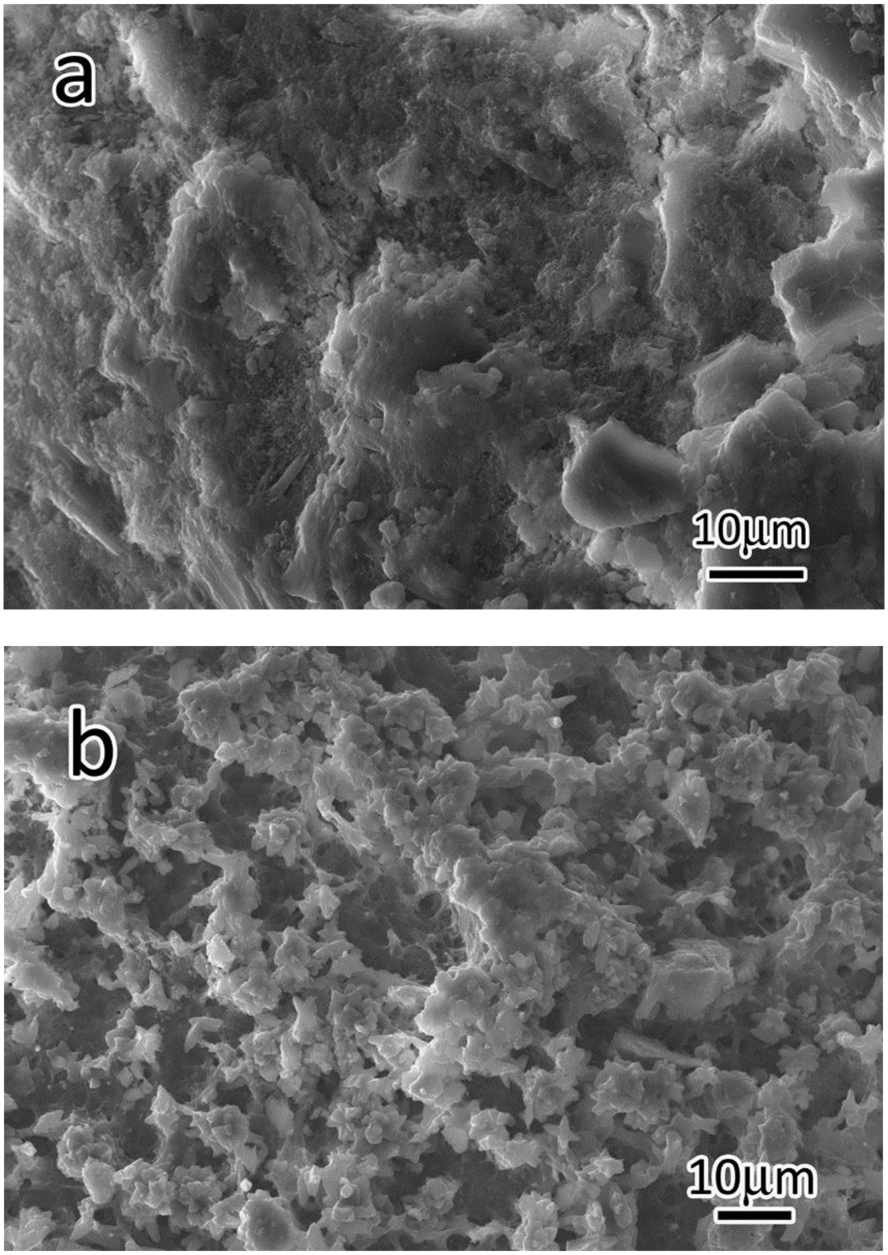
a
10µm
b
10µm

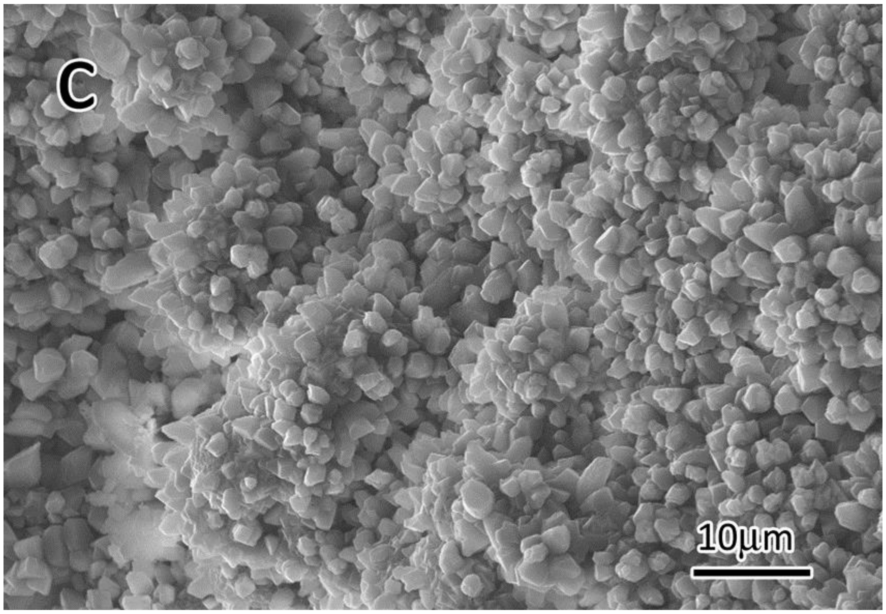

Fig. 5. 14 High magnification fracture surface SEM morphologies of the samples cored from site SR28, a) limited, b) moderate, and c) severe

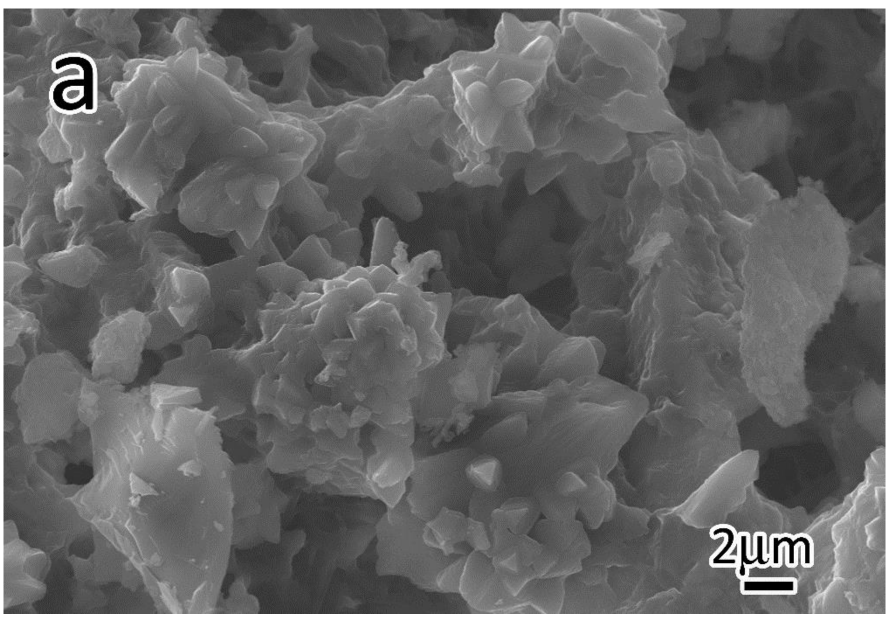

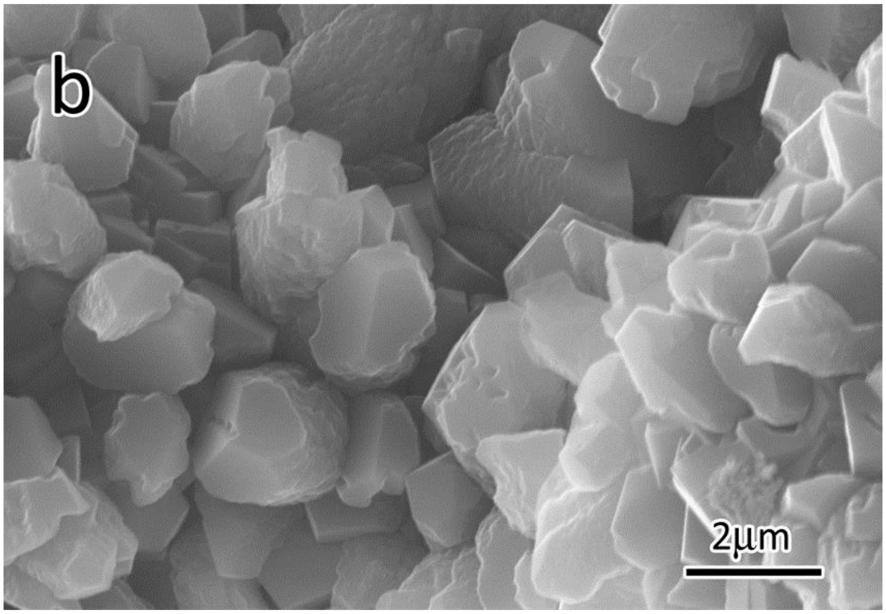

Fig. 5. 15 High magnification fracture surface SEM morphologies of the samples cored from site SR28, a) moderate, and b) severe

5.3.2 μCT

The 3D μCT results provide further proof of the microstructure changes with the samples cored from sites of SR28 and SR431. Different from the air voids content and water permeability testing, the resolution of the μCT is 10 μm; therefore, the porosities tested by the *μ*CT include multiscale pores, which is the key parameter that can determine the final properties of the concrete samples.

Fig. 5.16 and Fig. 5.17 show the typical 2D microstructures of the samples cored from SR28 and SR431. As shown in these figures, the content of the pores is evidently lower in the samples from SR28 than those from the SR431.

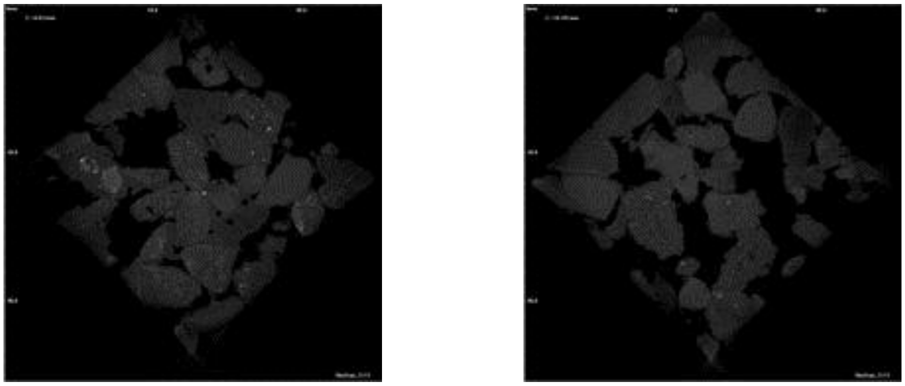

Fig. 5. 16 Typical μCT images of the sample cored from SR28

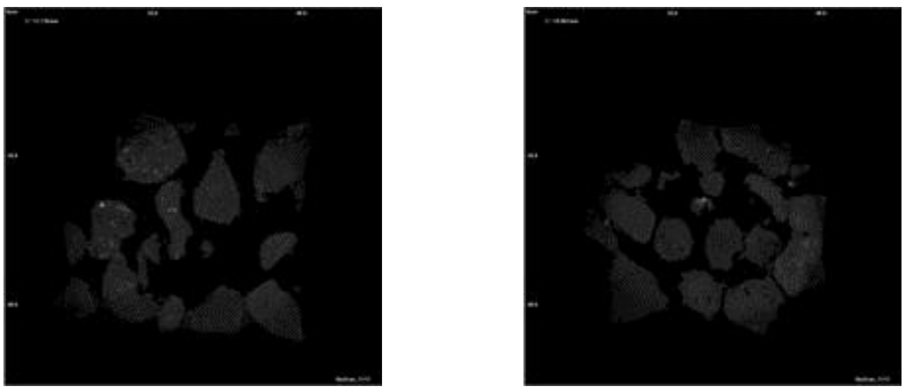

Fig. 5. 17 Typical μCT images of the sample cored from SR431

The porosity results calculated from the 3D μCT testing results are listed in Table 5.3. The findings show that the porosity of the sample from site SR28 is lower than the porosity of the sample from site SR431, with values of 31.4% and 47.2%, respectively.

By comparing with the air voids content data, the 3D μCT testing results show similar results, specifically that the SR28 samples have a lower porosity than the SR431 samples. However, by testing the pore size in multiscale, the porosity difference between them evidently increased from 5% to 50%. It means that the SR431 samples have 45% more micropores than the SR28 samples. This is the main reason that the mechanical properties of the samples cored from site SR431 are lower than the samples cored from site SR28.

Table 5. 3 Porosity tested from 3D μCT of the samples cored from SR28 and SR431

Sample No.	Porosity
SR28	31.4%
SR431	47.2%

There are several possible factors that will result in the considerable microstructure variations. First, the maintenance activities such as deicer impact had a strong chemical effect on the cement binder phase morphologies. The more deicer exposure, the higher chemical reaction degree will occur between the deicers and the cement binder phase. Second, the freeze/thaw damages during the winter season will lead to a serious physical damages of the cement binder phase. This can also be detected by SEM images and the μCT results. Third, the implementation process also had a straight influence on the final microstructures of the cement binder phase. The water/cement ratio is a key factor that affects the final properties of the concrete. Pervious concrete has a relatively high porosity, so it is very hard to precisely control a homogeneous water/cement ratio in all areas. As a result, the water/cement ratio might be considerably different in samples from various locations. In addition, the surface condition of the aggregates is another important factor that determines the final performance of pervious concrete pavements.

5.5 Key findings

- The compressive strength of the samples cored from SR28 is about 20% higher than the samples cored from SR431, while the splitting tensile strength is about 50% higher.
- The abrasion resistance of the samples cored from SR28 is about 20% higher than those from SR431.
- The samples cored from SR28 show slightly higher density and lower air voids content than the samples cored from SR431.
- The samples cored from SR28 have about 20% hydraulic conductivity than those from SR431.
- The samples cored from SR28 have about 50% lower water absorption than those from SR431. The water absorption results in conjunction with the hydraulic conductivity results suggest that the microstructure and micro-porosity of the samples cored from these two sites are largely different.
- The samples cored from SR28 show a better resistance to salt scaling than the samples cored from SR431. After seven freeze/thaw cycles in the 3% sodium chloride solution, the mass losses of SR28 samples are 27.24% and 81.07%, while the losses from the SR431 samples are 90.35% and 89.77%.

- The μCT analysis shows that the micrometer-scale porosity of the samples cored from SR28 is much lower than those from SR431.
- The observed SEM images of the fracture surfaces of the samples cored from SR28 and SR431 demonstrate that the *limited* distress samples show a well-maintained cement binder phase. In contrast, the *moderate* distress samples show some needle-shaped precipitates embedded in the cement binder phase. The predominant phase of the *severe* distress samples consists of a large number of micro-sized crystalline precipitates, instead of cement binder phase.
- The specific mechanism responsible for the premature failure of pervious concrete remains unclear and merits further investigation. One hypothesis to test is that the distresses observed in pervious concrete originated from the construction practice, e.g., insufficient compaction at some locations, and later aggravated by the exposure to freeze/thaw cycles, deicers, and mechanical loading in the service environment. Enhanced understanding of the failure mechanisms would help guide better design, construction, and maintenance practices for pervious concrete.

5.6 References

ASTM. 2012. Standard Test Method for Compressive Strength of Cylindrical Concrete Specimens. ASTM standard C39/C39M. American Society for Testing Materials, West Conshohocken, PA.

ASTM. 2011. Standard Test Method for Splitting Tensile Strength of Cylindrical Concrete Specimens. ASTM standard C496/C496M. American Society for Testing Materials, West Conshohocken, PA.

ASTM. 2012. Standard Practice for Capping Cylindrical Concrete Specimens. ASTM standard C617/C617M. American Society for Testing Materials, West Conshohocken, PA.

ASTM. 2006. Standard Test Method for Density, Absorption and Voids in Hardened Concrete. ASTM standard C642. American Society for Testing Materials, West Conshohocken, PA.

ASTM. 2012. Standard Test Method for Scaling Resistance of Concrete Surfaces Exposed to Deicing Chemicals. ASTM standard C672/C672M. American Society for Testing Materials, West Conshohocken, PA.

ASTM. 2011. Standard Test Method for Determining Potential Resistance to Degradation of Pervious Concrete by Impact and Abrasion. ASTM standard C1747/C1747M. American Society for Testing Materials, West Conshohocken, PA.

ASTM. 2012. Standard Test Method for Density and Void Content of Hardened Pervious Concrete. ASTM standard C1754/C1754M. American Society for Testing Materials, West Conshohocken, PA.

Huang, B., H. Wu, X. Shu, and E.G. Burdette. 2010. "Laboratory Evaluation of Permeability and Strength of Polymer-Modified Pervious Concrete" *Constr. and Build. Mat.*, 24(5), 818–823.

McCain, G.N., M.J. Suozzo, M.M. Dewoolkar. 2010. "A Laboratory Study on the Effects of Winter Surface Applications on the Hydraulic Conductivity of Porous Concrete Pavements" Transportation Research Board 2010 Annual Meeting CD-ROM.

Montes, F., S. Valavada, L.M. Haselbach. 2005. "A New Test Method for Porosity Measurements of Portland Cement Concrete" *J. of ASTM Int'l*, 2(1), January, 13pp.

Rizvi, R., S. Tighe, V. Henderson, J. Norris. 2010. "Evaluating the Use of Recycled Concrete Aggregate in Pervious Concrete Pavement" *Transportation Research Record No. 2164*, 132-140.

Schaefer, V.R., K. Wang, M.T. Suleiman, and J.T. Kavern. 2006. Mix Design Development for Pervious Concrete in Cold Weather Climates. Iowa DOT Final Report No. 2006–01.

Chapter 6 Conclusions

Pervious concrete has been increasingly used as a powerful tool to mitigate negative impact on the environment. It has many advantages for urban cities, including stormwater runoff management, traffic noise control, groundwater recharge, and mitigation of the urban heat island. The various mixes proportions can produce a wide range of properties in pervious concrete pavement, and various additives are helpful to enhance the overall performance of pervious concrete materials. In general, it is hard to optimize both the mechanical properties and the infiltration performance of the pervious concrete at the same time; therefore, new technologies need to be developed to help increase the mechanical properties without largely sacrificing the infiltration properties. In addition, the freeze/thaw damages, deicer impacts, and clogging phenomenon still create bottleneck problems for pervious concrete pavements. Besides the practical problems, the ongoing designing challenges include quantitative characterization of the pervious concrete materials and the quantitative relationship between the pore structures and the performance of the pervious concrete.

In the summer of 2012, NDOT constructed a pervious concrete pavement near Lake Tahoe. Specifications for this installation included a 7″ thick pervious concrete pavement surface over an 8″ thick aggregate drainage layer and 6″ thick geotextile-encapsulated sand bed. Two pervious concrete were installed at SR 431 and SR 28. The field testing results show that the slump of the freshly mixed pervious concrete was 1/4 inch, the unit weight was 123.2 PCF, the total air voids was 22.8%, the average 7d and 28d compressive strengths were 2770 and 3330 psi, respectively, and the average 7d and 28d tensile strengths were 300 and 315 psi, respectively. The freshly mixed pervious concrete has an average infiltration rate of 0.3-0.4 in/sec; however, after one year service, the infiltration rate was reduced to 0.1-0.01 in/sec.

The engineering performance and microstructure analysis of the samples cored from the fields were tested in the laboratory. The compressive strength of the samples cored from SR28 is about 20% higher than the samples cored from SR431, while the splitting tensile strength is about 50% higher. The abrasion resistance of the samples cored from SR28 is about 20% higher than the samples cored from SR431. The density and air voids testing results show that the samples cored from SR431 and SR28 have similar values. The samples cored from SR28 shows slightly higher density and lower air voids content and the samples cored from SR431. The hydraulic conductivity testing results show that the samples cored from SR28 has about 20% lower value than those from SR431. The water absorption testing results demonstrated that the samples cored from SR28 have about 50% lower value than those from SR431. The water absorption results in conjunction with the hydraulic conductivity results suggest that the microstructure and micro-porosity of the samples cored from these two sites are largely different. The samples cored from SR28 shows a better freeze/thaw resistance than the samples cored from SR431. After 7 freeze/thaw cycles in the 3% sodium chloride solution, the mass loss of SR28 samples are 27.24% and 81.07%, while the SR431 samples are 90.35% and 89.77%. The □CT analysis shows that the micrometer-scale porosity of the samples cored from SR28 is much lower than those from SR431.

A forensic investigation was conducted to shed light on the premature raveling of some pervious concrete segments. The observed SEM images of the fracture surfaces of the samples cored from SR28 and SR431 demonstrate that the *limited* distress samples show a well-maintained cement binder phase. In contrast, the *moderate* distress samples show some needle-shaped precipitates embedded in the cement binder phase. The predominant phase of the *severe* distress samples consists of a large number of micro-sized crystalline precipitates, instead of cement binder phase. One hypothesis to test is that the distresses observed in pervious concrete originated from the construction practice, e.g., insufficient compaction at some locations, and later aggravated by the exposure to freeze/thaw cycles, deicers, and mechanical loading in the service environment. Enhanced understanding of the failure mechanisms would help guide better design, construction, and maintenance practices for pervious concrete.